

162-15135

NASA TN D-1314

NASA TN D-1314



11

TECHNICAL NOTE

D-1314

BOILING HEAT TRANSFER TO LIQUID HYDROGEN
AND NITROGEN IN FORCED FLOW

By James P. Lewis, Jack H. Goodykoontz,
and John F. Kline

Lewis Research Center
Cleveland, Ohio

NATIONAL AERONAUTICS AND SPACE ADMINISTRATION
WASHINGTON

September 1962

NATIONAL AERONAUTICS AND SPACE ADMINISTRATION

TECHNICAL NOTE D-1314

BOILING HEAT TRANSFER TO LIQUID HYDROGEN
AND NITROGEN IN FORCED FLOW

By James P. Lewis, Jack H. Goodykoontz,
and John F. Kline

SUMMARY

Boiling heat transfer to liquid hydrogen and nitrogen was investigated experimentally. Results are presented from a study of bulk boiling inside a cylindrical tube under vertically upward forced-flow conditions. A 0.555-inch-inside-diameter and $16\frac{1}{8}$ -inch-long electrically heated stainless-steel tube was used. The range of variables studied for hydrogen were mass velocity of 2850 to 17,000 pounds per hour per square foot, local heat flux of 3600 to 40,000 Btu per hour per square foot, inlet pressure of 30 to 74 pounds per square inch absolute, and inlet subcooling of 0° to 9° R. Nitrogen test conditions were mass velocity of 15,000 to 56,000 pounds per hour per square foot, local heat flux of 2300 to 40,000 Btu per hour per square foot, inlet pressure of 47 to 56 pounds per square inch absolute, and inlet subcooling of 1° to 6° R.

The axial distribution of the tube-wall temperatures is presented. A transition in the type of boiling heat transfer was obtained. The critical heat flux corresponding to this transition was determined over a range of flow and heating rates and local qualities. At specific combinations of flow and transition location, a range of critical-heat-flux values was obtained and maximum values were determined. The maximum critical heat flux increased with increasing fluid-flow rate and decreased with increasing length of tube before transition. Similar variations of the maximum critical heat flux have been reported for water. The tube-inner-wall temperatures upstream of transition were essentially uniform and were only slightly greater than the fluid saturation temperature. The wall-temperature profiles downstream of transition generally resembled those obtained in film-boiling studies and appeared to be strongly dependent upon local quality at the point of transition. Maximum wall temperatures of 900° and 1800° R were obtained with hydrogen and nitrogen, respectively. Fluctuations of pressure, flow rate, and temperature occurred during some of the boiling tests. Under some conditions, maximum critical-heat-flux values were attained during steady-state operation with fluctuations. In other cases the fluctuations became uncontrolled, and critical-flux values less than the maximum values were obtained upon restabilization of the test conditions. No measurable pressure drop across the test section was obtained at any condition.

INTRODUCTION

Liquid hydrogen has been proposed for use in several advanced propulsion systems. In these systems, hydrogen may be used both as a propellant and as a coolant. The low boiling point of hydrogen and the desirability of storing it in the liquid state in addition to the requirements of some systems for gaseous hydrogen necessitate a knowledge of two-phase flow and heat transfer for hydrogen. Information is especially desired for boiling heat transfer of hydrogen under forced-flow, confined-geometry conditions. In addition, the wide variance of the physical properties of hydrogen from those of more conventional fluids make it attractive as a test fluid in research directed towards a more complete understanding of the general problem of boiling heat transfer.

Information in the literature concerning boiling heat transfer, primarily for the case of pool (or pot) boiling and usually for conventional fluids, such as water and alcohols, is extensive. Present thinking with respect to pool boiling and related investigations with hydrogen are summarized in reference 1. Pool boiling is characterized by three distinct modes of boiling, namely, nucleate, transition, and film boiling. Analytical and empirical relations between the heat flux (or heat-transfer coefficient) and the wall- to fluid-temperature difference have been obtained for pool boiling. Pool boiling also exhibits a distinctive value of heat flux obtained at the boundary between the nucleate and transition boiling regions that has been variously termed maximum nucleate flux, departure from nucleate boiling (DNB), or burnout heat flux. Analytical and experimental correlations of the maximum nucleate flux with fluid properties and test operating variables have been made with varying degrees of success (ref. 1).

For the case of forced flow in confined geometries, the current understanding of boiling heat transfer is much more limited, especially for the case of net vapor generation. Again, considerable data have been obtained and several correlations have been proposed (refs. 2 to 6). Much of the available data are incompletely presented or contradictory, and the correlations, which successfully relate the results of a single study, have not been successful when applied to other tests or fluids of widely differing properties. The experimental data of several investigations (refs. 2 to 4) have indicated the existence of a critical heat flux, which somewhat resembles the maximum nucleate flux obtained in pool boiling, in that a well defined reduction in the heat-transfer coefficient is obtained. Some data of this type that resemble the usual results obtained for pool boiling were obtained in limited tests of boiling hydrogen (ref. 7). Data were obtained in reference 8 for hydrogen for the region that might be termed film boiling in tubes with forced flow. For the investigations of boiling heat transfer with forced flow in confined geometries, there is a wide variation in the assumptions regarding the physical nature of the heat-transfer process and in the definition of the critical heat flux.

Because of the aforementioned limitations of present knowledge, a program was initiated at the Lewis Research Center to investigate boiling heat transfer to liquid hydrogen under conditions of forced flow inside a vertical tube. The principal objective of the investigation was to determine in engineering terms the effect of the operating variables (flow rate, pressure, liquid inlet subcooling, heating rate, and tube geometry) on the mode of heat transfer and their relation to the value of the critical heat flux. The program was directed towards conditions resulting in net vapor generation. In addition, information on flow instability and its effect on heat transfer were desired.

The test apparatus consisted of a pressure-fed, once-through system with an electrically heated vertical tube of 0.555-inch inside diameter and $16\frac{1}{8}$ -inch length. Both subcooled liquid para-hydrogen and liquid nitrogen flowed through the tube in vertical upflow. The range of variables investigated was limited to the following:

	Hydrogen	Nitrogen
Mass velocity, lb/(hr)(sq ft)	2850 to 17,000	15,000 to 56,000
Local heat flux, Btu/(hr)(sq ft)	3600 to 40,000	2300 to 40,000
Liquid inlet subcooling, °R	0 to 9	1 to 6
Inlet pressure, lb/sq in. abs	30 to 74	47 to 56

Tube-exit qualities ranged from essentially 0 to 1.0 (with superheat), and transition from a relatively high to a lower value of heat-transfer coefficient occurred over a range of axial locations from tube entrance to exit. A few tests were made with cold hydrogen gas flowing through a heated tube. The results obtained from the investigation are presented in tabular and graphical form.

APPARATUS

General Arrangement

The test equipment included a liquid-supply Dewar, a controlled source of pressurizing gas, a flash cooler to subcool inlet test liquid, the test section and electric power supply, inlet and exit control valves, a vaporizer, an orifice-type flowmeter, and vent, pressure relief, and purge systems (fig. 1). In practically every case, the test liquids (para-hydrogen and nitrogen) were pressurized by their own gases. Gaseous helium was used for system purging and inerting. The vaporizer was used to ensure that only a fully vaporized product would pass through the flow orifice. All fluid lines from the supply Dewar to a point past the end of the test section were insulated with a vacuum jacket.

Test Section

The test-section assembly consisted of the electrically heated tube, inlet and outlet chambers, a vacuum jacket, and test instrumentation (fig. 2). The tube was made of type 304 stainless steel with a 0.555-inch inside diameter and a 0.035-inch-thick wall. As indicated in figure 2, the effective heated length of the tube was $16\frac{1}{8}$ inches, measured between the inner faces of the end flanges. All distances along the tube from the tube inlet were measured from the downstream side of the inlet flange. The actual inlet end of the tube extended $1/2$ inch upstream of this point. The inlet chamber consisted of a $1\frac{1}{2}$ -inch-inside-diameter stainless-steel cylinder attached to the inlet flange. The inlet chamber, which was lined with $1/8$ -inch-thick thermal insulation, was designed to provide a low-velocity plenum at the test-section entrance and to minimize heat leakage from the heated test section to the incoming liquid. Two copper bus bars, diametrically opposite, were connected between the test-section inlet flange and the bottom flange of the vacuum jacket, which also served as the ground side of the electrical circuit. These bus bars were 4 inches long with a cross section of $1/8$ by 1 inch. The outlet chamber was designed to minimize heat losses from the tube, to provide an electrically insulated, low-electrical-resistance connection to the tube, and to provide a thermally insulated mixing chamber, in which the test fluid could come into thermal and phase equilibrium. The outlet chamber contained an inner liner consisting of stainless steel and Teflon. This liner, which was not attached directly to the tube, was designed to allow cool gas to accumulate between it and the outer shell and thus to act as thermal insulation. The outlet section was connected to a 1-inch-outside-diameter copper tube that passed through the vacuum jacket and was electrically isolated from it. Two conically shaped mixing screens were placed in the outlet section. The vacuum jacket around the test-section assembly consisted of stainless-steel flanges with O-ring seals, a $3\frac{1}{2}$ -inch-diameter Lucite tube, and an aluminum-foil radiation shield.

Flash Cooler

The flash cooler shown in figure 1 was provided to supply subcooled liquid to the test section. The cooler consisted basically of three concentric tubes. The flow of the liquid to the test section was brought through the small innermost tube. Some liquid was allowed to pass into the annular space around the inner tube through bleed holes at various points along the length of the subcooler. The pressure in this annulus was maintained intermediate between atmospheric pressure and the supply Dewar pressure by a throttle valve. The liquid entering the annular

space vaporized because of the drop in pressure and thus cooled the inner supply tube. The inner tube had a 0.38-inch outside diameter with a 0.032-inch wall. Stainless-steel rods, 1/4 inch in diameter, were inserted into the inner tube to promote cooling of the supply liquid. The outer annular space provided a vacuum jacket for thermal insulation.

Electric Power Supply

The tube was heated by alternating current supplied through a $2\frac{1}{2}$ -kilowatt, 60-cycle transformer with a maximum current rating of 500 amperes. The power to the test section was controlled by a variable autotransformer in the primary circuit. The current to the test section was measured by a laboratory-quality ammeter connected to a current transformer with a ratio of 100. Voltage drops across the tube at various locations were measured with a Ballantine vacuum-tube voltmeter.

Instrumentation

Instrumentation was provided to measure the inlet and the exit fluid bulk temperatures, the tube-wall temperatures, the inlet-fluid pressure, and the test-fluid flow rate.

Fluid temperatures. - The fluid bulk temperatures were measured by carbon resistors in the inlet and the exit of the test section (see fig. 2). The carbon resistors at the test-section outlet were located both above and below the mixing screens. The carbon resistors were hermetically sealed in a protective sheath about 0.1 inch in diameter by 0.2 inch long. The carbon resistors acted as one arm of a bridge circuit, the output of which was recorded on a self-balancing potentiometer. The slope of the temperature-resistance curve was obtained in a laboratory calibration and was essentially invariant. Shifts of the curve occurred, however, that required daily adjustment with a trimming resistance at a known temperature condition. The fluid temperature at the orifice flowmeter was measured with a copper-constantan thermocouple. The overall accuracy of the fluid bulk temperatures is estimated at approximately $\pm 0.5^\circ$ R.

Wall temperatures. - The temperatures of the tube wall and of adjacent sections were obtained with copper-constantan thermocouples. The thermocouples were soldered to the outside of the tube wall and the leads were wrapped around the tube several times and were finally wrapped with glass-fiber tape. The tube-wall thermocouples were positioned in one longitudinal plane and their axial locations are given in table I. The positions of the thermocouples that were installed on the inlet section, the outlet section, and the ground bus are also given in table I. These thermocouples were used to monitor the flow of heat to and from the test section.

The constantan wire from each thermocouple junction was led without interruption to individual reference junctions located in a liquid-nitrogen bath at atmospheric pressure. Copper leads led from the bath to a manual selector switch. The thermocouple voltage was bucked by a 1-millivolt voltage to obtain positive values, and the resultant signal was recorded on a self-balancing potentiometer. The calibration of the thermocouples was determined from the National Bureau of Standards calibration (ref. 9) and laboratory calibration checks. The calibration indicated a very low sensitivity for the copper-constantan thermocouples near liquid-hydrogen temperatures. Wall temperatures, however, were obtained from approximately 40° to 1800° R. Above 1200° R, an extrapolation of the curve of reference 9 was used. The sensitivity and accuracy of the thermocouple readings are indicated by the following table:

	Liquid-hydrogen temperature (45° R)	Liquid-nitrogen temperature (160° R)	Room tempera- ture (530° R)
Sensitivity, mv/°R	0.004	0.01	0.022
Chart reading limit, mv	0.01 to 0.02	0.01 to 0.02	0.01 to 0.02
Chart reading limit, °R	2.5 to 5	1 to 2	0.5 to 1

The thermocouple calibration points also showed a scatter of approximately $\pm 3^\circ$ R at liquid-hydrogen temperatures and $\pm 1^\circ$ R at liquid-nitrogen temperatures. Approximately the same scatter was obtained from the actual tube-wall thermocouples during no-heat runs. The tube-wall thermocouples were attached to the outside of the tube wall. The temperature of interest, however, is that of the inner surface. An analysis and computation of the temperature drop through the tube wall is given in appendix A for the case of negligible axial temperature gradients. This analysis indicates wall drops of up to 20° R for liquid-hydrogen conditions and up to 7° R for liquid-nitrogen conditions over the range of the test heat fluxes.

Pressure. - The fluid pressures were sensed with strain-gage-type transducers and were continuously recorded on a high-speed recording potentiometer (0.3-sec full-scale travel). Pressure was sensed at the test-section inlet (see fig. 2) by a transducer having a range of 0 to 100 pounds per square inch absolute and an overall accuracy of ± 0.5 percent of full scale. Initially a differential pressure transducer was installed to measure the pressure drop across the test section. Since no measurable pressure drop was obtained at the largest flow and vaporization conditions, the downstream pressure tap was removed to aid in eliminating flow and pressure oscillations. The fluid pressure far downstream of the tube exit (upstream of the exit control valve) was monitored on a visual gage but showed no significant drop from the test-section inlet pressure. The pressure in the flash cooler was also sensed by a strain-gage transducer.

Flow rate. - The test-fluid flow rate was measured by a sharp-edge orifice downstream of the vaporizer. The vaporizer ensured that all the fluid was in the gaseous phase and at a temperature at which fluid properties are well known. The discharge coefficient was determined with water for a range of Reynolds numbers. The orifice pressure and pressure drop were measured with strain-gage-type transducers and recorded on a self-balancing potentiometer. The flow-rate measurements are estimated to have an accuracy of ± 2 percent.

PROCEDURE

Establishment of Test Conditions

Obtaining information on boiling heat transfer for various heating rates at several pressure levels and over a range of flow rates in a systematic way was desired in order that the effects of each variable could be determined. It was also desired to have the test liquid enter the test section slightly subcooled and to study heat transfer and two-phase flow in forced flow over as great a range of fluid quality as possible and to obtain a critical heat flux at arbitrary locations along the tube axis. (The critical heat flux is defined as the flux immediately before the transition from the high upstream heat-transfer coefficient to a lower value.) Completely systematic operation was not always possible because of limitations of the test equipment and of the boiling process itself. In addition, operation at a precise preselected condition was difficult to attain because of fluctuations of flow and pressure that occurred in the system.

The general operating procedure consisted of setting conditions of flow rate, pressure, and inlet subcooling without heat addition and then gradually increasing the heat to the test section in small increments until the desired condition was obtained. As heat was added to the system, the flow and pressure conditions changed and had to be continually readjusted. The most consistent and repeatable results were obtained by always increasing the heat control setting and/or decreasing the flow rate. The range of test variables for the investigation of boiling heat transfer were test-section pressure, 30 to 74 pounds per square inch absolute; mass velocity, 2850 to 17,000 pounds per hour per square foot for hydrogen and 15,000 to 56,000 pounds per hour per square foot for nitrogen; inlet subcooling of 0° to 9° R for hydrogen and 1° to 6° R for nitrogen. The heated-tube-wall temperatures varied from 36° to 1800° R. The point of transition from a high to a lower heat-transfer coefficient was obtained at various locations along the length of the tube. Occasional unheated runs were made before and after a heated run. For an unheated run made after a heated condition, the flow and pressure controls were left unchanged in order that the effect of boiling on the flow conditions might be studied. A few runs were made in which cool hydrogen gas flowed through the tube at nominal pressures of 50 and 70 pounds per square inch absolute, inlet temperatures of 46°

to 82° R, and mass velocities of 7800 to 13,000 pounds per hour per square foot.

Data Reduction and Computations

All wall temperatures were obtained from the thermocouple chart readings and the aforementioned copper-constantan thermocouple calibration. Inner-tube-wall temperatures for a negligible axial temperature gradient were obtained from the calculations of appendix A. All pressures were read directly from the recorder charts. The flow rate was computed by the standard ASME orifice equations. Fluid properties were taken primarily from National Bureau of Standards sources (refs. 9 and 10).

The local heat flux was computed from the measured current and tube-outer-wall temperature by equation (All).

The local vapor quality was obtained from a heat balance by the relation

$$x = \frac{Q - wc_p(t_{\text{sat}} - t_{\text{in}})}{wh_{\text{fg}}} \quad (1)$$

(All symbols are defined in appendix B.) For the special case of negligible axial temperature gradient (hence, constant heat flux), the quality is given by

$$x = \frac{4 \left(\frac{q}{G} \right) \left(\frac{L}{D} \right) - c_p(t_{\text{sat}} - t_{\text{in}})}{h_{\text{fg}}} \quad (2)$$

Heat balances were computed for a few cases by comparing the enthalpy rise of the fluid through the test section with the amount of electric heat supplied to the test section. The heat balance could be computed only for cases with subcooled inlet liquid and superheated exit vapor (except for the hydrogen-gas runs) because there was no independent means of measuring quality. The heat balances agreed in most cases within ± 10 percent. Usually the heat input was greater than the measured increase in fluid enthalpy, which indicated a heat loss. The main sources of heat loss (or gain) are the vacuum jacket, the copper ground bus, and the inlet and the exit sections. Calculations indicated that heat transfer across the vacuum jacket to the test section was negligible. Conduction through the copper ground bus was into the inlet section and was less than 5 percent of the heat generated in the tube. The heat loss from the tube through the walls of the inlet section was less than 2 percent of the heat generated in the tube. Evaluation of the heat loss at the exit of the test section was impossible. An additional source of error arose from the possible nonequilibrium of temperature and the phase of the test

fluid at the points of measurement in the inlet and the exit sections. The heat balance, however, was satisfactory and within the accuracy expected from the individual measurements.

RESULTS AND DISCUSSION

Tabulation of Data

The data obtained in 160 separate runs are tabulated in table II. Included in the table are data for runs both with liquid hydrogen and with liquid nitrogen, both heated and unheated, and also heated and unheated gaseous-hydrogen runs. The original data consisted primarily of the tube-outer-wall temperatures and the fluid exit bulk temperature obtained for various tests conditions of pressure, inlet fluid temperature, flow rate, and heating rate. For cases in which significant fluctuations of tube-wall temperatures occurred, the magnitudes of such fluctuations are also tabulated. The runs are numbered in chronological order. An omission in the run-number sequence indicates an aborted run or a significant change in the testing program. Also presented in table II are the temperatures measured on the electrical ground bus and in the inlet and the outlet sections. The table also contains the calculated values of the fluid inlet subcooling, the fluid exit superheat, the critical heat flux (or the uniform flux on the tube if it is below the critical value), the position of the point of transition in heat transfer (termed the critical-boiling-length-to-diameter ratio), and the local quality at the point of transition (termed the critical quality). The remarks tabulated for each run are based on observations made during the test and also on subsequent study of the data.

Tube-Wall Axial-Temperature Profiles

The tube-outer-wall temperature profiles along the length of the tube for liquid-hydrogen tests at a pressure of approximately 50 pounds per square inch absolute and an average inlet subcooling of 2°R are presented in figure 3 for various heating rates at two different nominal mass velocities. Also included in the figure are the temperatures of the inlet and the outlet sections and a schematic diagram of the test-section geometry, including thermocouple locations. All the profiles of figure 3 have the same general shape but show trends with respect to heating rate and mass velocity. Starting at the tube inlet, the wall temperatures are essentially constant until a sudden temperature rise is obtained at various downstream locations. Following the initial sharp rise, the slope of the temperature profile decreases and in some cases the curves appear to approach a constant temperature. Listed in figure 3 are the values of the local heat flux existing immediately upstream of the

point of temperature rise. This heat flux, arbitrarily termed the critical heat flux, is indicative of a boiling heat-transfer condition at which, for a given flow and pressure, a transition occurs from a relatively large heat-transfer coefficient to a smaller coefficient at a specified position along the tube axis. (The flux downstream of the transition point is larger than the critical flux because of the increase in tube electrical resistance, but the proportionate increase in flux is much less than the increase in wall temperature.) The critical flux may not correspond to the maximum nucleate or burnout flux obtained in pool boiling; for the terms to be synonymous, evidence would be required that the critical heat flux results from surface ebullition.

All the data of figure 3 show an increase in the critical heat flux as the location of transition moves upstream. This inverse relation was also found in tests with water for transition occurring at the exits of tubes of various lengths (ref. 4). The temperature-rise curves for the nominal mass velocity of 12,000 pounds per hour per square foot (fig. 3(a)) show a more pronounced change in slope and tend to approach a constant value of temperature sooner than those for the lower flow rate (fig. 3(b)). These effects are probably related to the lower qualities at the critical point obtained at the higher flow rate; however, a difference in the two-phase flow pattern (void-fraction distribution) is felt to be the controlling factor.

All the wall temperatures of figure 3 upstream of transition are uniform along the tube within the limits of the instrumentation and show a small and nonsystematic variation between runs. The inner-wall temperatures can be obtained by subtracting the wall-temperature drop (given in appendix A) from the outer-wall temperatures of figure 3. The inner-wall temperatures are approximately 12° and 3° R above the inlet fluid saturation temperature for the conditions of figures 3(a) and (b), respectively. These small temperature differences are not considered accurate enough for further analysis because of the inherent inaccuracy and lack of sensitivity of the temperature measurements at these low temperatures (40° to 70° R).

Since the highest wall temperatures obtained with hydrogen never exceeded 900° R and in most cases were less than 600° R, safe operation over a considerable range of conditions in a region equivalent to film boiling with forced flow seemed possible. Similar magnitudes of wall temperature were obtained in reference 8.

The tube-wall temperature profiles obtained with liquid nitrogen as the test fluid were generally similar to the results with hydrogen. (All nitrogen data are given in table II(b).) The rise in wall temperature following transition was much steeper for nitrogen than for hydrogen and the high temperatures (up to 1800° R) obtained finally caused failure of the test apparatus. During operation with liquid nitrogen,

attempts to obtain transition upstream of the tube exit generally resulted in unstable conditions with extreme fluctuations of flow, pressure, and wall temperature.

A few tests were made in which cool hydrogen gas flowed through the heated tube. These tests were made to obtain tube-wall axial temperature profiles for conditions of gas convective heat transfer for comparison with the temperature profiles obtained with boiling heat transfer. The profiles shown in figure 4 are for turbulent convective heat transfer and are considerably different from those obtained with boiling heat transfer (fig. 3). For the convective heat transfer, the tube-wall rise always started close to the tube inlet and the wall-temperature rise was generally more gradual than for the boiling heat-transfer tests. The shape of the convective wall-temperature profiles results primarily from entrance effects and variations in the tube-wall- to fluid-bulk-temperature ratio. The shape of the wall-temperature profiles for the boiling case (fig. 3), however, reflects changes in phase and in the boiling heat-transfer mechanism.

Temperature profiles are presented in figure 5 for boiling hydrogen at two constant values of transition location for several values of mass velocity and critical heat flux. An increase in mass velocity tends to skew the temperature-rise curves by increasing the slope at first and then by decreasing it at downstream locations. This effect of mass velocity on the temperature-rise curves was previously shown by the data of figure 3.

Critical Heat Flux

The critical heat flux for the conditions of this investigation corresponds to the local heat flux just upstream of the location of a sudden rise in wall temperature. For the critical heat flux at the end of the tube, transition was defined as the point corresponding to the conditions existing just previous to the increase in flux that first caused the thermocouple located 1/2 inch from the tube exit to rise. The critical heat flux obtained for boiling liquid hydrogen at a pressure of approximately 50 pounds per square inch absolute is presented in figure 6 as a function of mass velocity for four nominal values of the critical-boiling-length-to-diameter ratio L/D . All these curves show a significant increase in the critical flux with increasing mass velocity, but the slope of the curves generally decreases with increasing mass velocity. Generally the critical flux increases as the L/D decreases for constant mass velocity. Similar relations were found for water in reference 4, in which transition occurred at the exit of tubes of various lengths and diameters. In the present investigation, the length variation was obtained by causing transition to occur at various locations along a tube of constant length and diameter. The data of figure 6 show

an increased scatter with reduction in the critical L/D . The points of greatest heat flux in figure 6(d) also had the greatest fluctuations of wall temperature, flow rate, and pressure but were essentially steady-state conditions. The points along the lower envelope of critical flux in figure 6(d) did not show any fluctuation. Some of these lower points were obtained by deliberately overheating and then decreasing power and/or by increasing the flow rate until a stable condition was obtained. The rest of the lower points were obtained by a similar, but uncontrolled, process that could occur independently following a perturbation and that would eventually result in a stable condition. The highest flux values obtained at a given operating condition are arbitrarily termed the maximum critical heat fluxes. Throughout the investigation the maximum critical heat fluxes were generally associated with fluctuations of wall temperature, flow rate, and pressure, while the lower values of critical flux normally occurred without fluctuations. The scatter of the critical-flux values increased as the transition point moved upstream for the entire investigation with both liquid hydrogen and liquid nitrogen. The temperature profiles presented in figures 3 and 5 are from tests in which the maximum critical flux was obtained.

The temperature profile for a maximum-critical-heat-flux case is compared with the temperature profile obtained at a lower value of critical flux in figure 7. All other conditions of flow rate, pressure, and inlet subcooling are essentially the same. The main difference in the two profiles is a higher temperature level for the maximum critical flux case, which reflects the increased heating rate. The lower critical flux was obtained by deliberately overheating and then by cooling.

Tube-wall-temperature profiles for tests with critical heat fluxes less than the maximum are presented in figure 8 for an essentially constant mass velocity and various transition locations. For transition occurring at a value of L/D of less than 8 (axial distance L of about 4), the profiles each have a definite peak and a minimum as contrasted with the profiles for larger values of L/D and the profiles of figures 3 and 5.

Some runs were made with the wall-temperature rise occurring at or near the tube inlet. The resulting profiles are shown in figure 9 for two pressures and various mass velocities. Many of these curves have peaks and minimum points and in this respect are similar both to the profiles of figure 8 for values of L/D of less than 8 and to the profiles reported in reference 8. The shape of the curves of reference 8 was explained on the basis of an inlet end effect, a two-phase annular-flow model with the associated momentum pressure drop along the tube, and the attainment of "dry-wall" or "vapor-binding" conditions. In the tests presented herein, no measurable pressure drop across the test section was obtained, but dry-wall conditions could be attained. The data of figure 9 do not seem to indicate any significant effect on the critical

heat flux of the increase in pressure from 50 to 70 pounds per square inch absolute. Whether the critical-heat-flux values for the data of figure 9 should be classified as maximum or submaximum values is not known. Additional data for small values of transition length are necessary to resolve this question.

The critical-heat-flux data for hydrogen that are considered to be maximums are shown in figure 10 in logarithmic coordinates as functions of mass velocity for several critical L/D 's. Lines of constant quality of 1.00 and 0.50 computed from a heat balance are also indicated in figure 10. The general trend of the data is similar to that obtained for the boiling of water at low pressure (ref. 4). The water data indicated a change of slope or a knee in the curve of flux against mass velocity with the knee at a quality of approximately 0.50. The hydrogen data, however, do not exhibit any marked change in slope, particularly in the region of a quality of 0.50. The hydrogen data are fairly limited compared with the water data of reference 4. The hydrogen data can be extrapolated to higher and lower qualities in a manner which would show that a knee occurs in the quality range of 0.60 to 0.70. These same data are cross plotted against the critical-length-to-diameter ratio in figure 11, which shows the inverse relation between the critical heat flux and the critical L/D . This effect is greatest for high qualities. Extrapolating the curves to small critical values of L/D would indicate a small effect of L/D on the maximum critical flux. This condition makes it difficult to determine if the data shown in figure 9 represent maximum-critical-flux values.

The variation of the critical heat flux with mass velocity for boiling liquid nitrogen is presented in figure 12. The results are given for transition at the end of the tube only ($L/D = 29$). For smaller values of critical L/D , the critical heat fluxes that were obtained were less than those of figure 12 at corresponding operating conditions. For this reason, the critical fluxes obtained upstream in the tube with nitrogen are not regarded as maximum critical fluxes as defined herein. Attainment of such maximum critical fluxes at critical values of L/D of less than 29 would be difficult and would require an improved apparatus with respect to stability control and material temperature limits. The general trend of the data of figure 12 agrees with that for hydrogen at a similar critical value of L/D (fig. 10) but with the critical flux at a larger value of mass velocity at approximately the same quality. This result reflects the lower latent heat of vaporization of nitrogen compared with hydrogen.

The data of figure 12 are also plotted in figure 13 together with the critical-flux data obtained with critical values of L/D of less than 29. The dashed line in figure 13 represents a quality of 1.00 for L/D of 29. With the exception of one point, all the critical-flux data for the short L/D tests fall below that for L/D of 29. In addition,

the critical flux obtained upstream of the tube exit appears to be independent of the location of transition over a considerable range of L/D . The resemblance between figure 13 of this report and figure 4 of reference 4 should be noted. Figure 4 of the reference for water (ref. 4) showed that the presence of compressible volumes limited the stability of the system and caused low values of critical flux. A similar, though unknown, limitation of system stability apparently existed for the nitrogen tests with transition upstream of the tube exit.

Normalization of Critical-Heat-Flux Data

Previous investigators (refs. 2 to 4) have tried various means of correlating and normalizing critical-heat-flux results. These efforts have been primarily empirical approaches. In reference 4, a large amount of data was normalized for forced-flow boiling of low-pressure water by using parameters including tube diameter, tube length, and mass velocity. The maximum-critical-heat-flux data of the present investigation are presented in terms of the parameters of reference 4 in figure 14 and compared with the water data of reference 4. The cryogenic data appear to be successfully normalized into single curves for each fluid with an acceptable degree of scatter. The normalized curves for the three fluids have the same general trends and are separated in the order of their respective latent heats of vaporization. A similar normalization of the data is shown in figure 15 but with slightly different powers of the length and the diameter terms. The normalization of the data in figure 15 appears to be equally as good as that in figure 14. Selection of the correct correlating parameters seems difficult without a realistic model of the two-phase flow and heat transfer, particularly for the cases of qualities approaching 0 and 1.00.

Acceptance of the normalization of the critical-heat-flux data in the form of figures 14 and 15 would imply an effect of the critical boiling length on the critical heat flux in addition to that required by a heat balance. If the length term is assumed to have no other effect than that required by a heat balance, the critical-flux data should be normalized by a plot of the critical flux against the mass velocity divided by the critical-length-to-diameter ratio L/D ; that is, the critical heat flux is a unique function of the local critical quality for a given fluid. The hydrogen maximum-critical-heat-flux data is shown in this way in figure 16. The dashed line represents a quality of 1.00 for all length values. The scatter of the data in figure 16 is only slightly worse than in figures 14 and 15. The actual data scatter appears to be unsystematic with the possible exception of the smallest L/D conditions, for which the heat-flux values fall lower than the rest of the data. Similar trends were obtained with the water data of reference 4; that is, the fluxes for small L/D data were low. The failure of the small L/D data to correlate with the rest of the results in a graph such as

figure 16 may be attributed to several factors, in addition to questions concerning the validity of the choice of correlating parameters. These are: (1) The data at small critical values of L/D were the most difficult to obtain and had the greatest tendency towards instability; (2) at short lengths, heat transfer and two-phase flow equilibrium may not have been achieved; and (3) the data at small values of L/D may be reflecting entrance effects. The relation between the maximum critical heat flux and the critical length has therefore apparently not been completely determined. An additional complicating factor is involved in the selection of the correct critical length. The water tests of reference 4 had considerable inlet subcooling and would be expected to have an appreciable length of subcooled boiling, whereas, in the present investigation, the subcooling was negligible and bulk boiling occurred over nearly the entire length. Whether the effective length should be measured from the tube inlet or from the location at which the fluid bulk reaches the local saturation temperature is unknown. This problem is treated in reference 3 in a discussion of the use of quality as a correlating parameter for the critical heat flux.

Wall Superheat

A conventional method of presenting boiling heat-transfer data (especially for pool or pot boiling) is a graph of the heat flux against the wall superheat (wall temperature minus the fluid saturation temperature). Data for nitrogen are presented in this form in figure 17. These data include both the maximum-critical-heat-flux conditions and conditions below critical (no transition). Most of the data appear to fall on a single curve with no significant effect of mass velocity. Included in figure 17 are the predictions of reference 11 for nitrogen and of reference 5 for nitrogen and water. It is claimed in reference 5 that the method presented therein of predicting boiling heat fluxes applies to flowing systems as well as to nucleate pool boiling. The results shown in figure 17 should not be interpreted as supporting the analytical predictions or their application to flowing systems. The agreement may be fortuitous, especially because of the limited extent and accuracy of the nitrogen data. Similar graphs for the hydrogen data are not presented because of the poor sensitivity of the copper-constantan thermocouples at hydrogen temperatures. In fact, the sensitivity of the thermocouples for the nitrogen conditions is considered marginal. Analytical predictions indicate a wall superheat of 1° to 3° R for the range of the hydrogen test conditions. The experimental data show a wall superheat of the order of 10° R or greater. Attributing this lack of agreement entirely to limitations of the thermocouples appears difficult. The data of reference 7 for hydrogen do not fully correlate with the analytical predictions of references 5 and 11.

SUMMARY OF RESULTS

The results of the investigation of boiling heat transfer to liquid hydrogen and nitrogen in forced flow may be summarized as follows:

1. Boiling heat-transfer data (wall temperatures and heat fluxes) were obtained for bulk boiling of liquid hydrogen and nitrogen under forced flow upward inside an electrically heated tube. Data were obtained over ranges of flow and heating rates and pressures for small amounts of inlet subcooling. A limited amount of data was obtained with flowing cool hydrogen gas.

2. A transition in the type of boiling heat transfer was obtained. The critical heat flux corresponding to this transition was determined over a range of flow and heating rates and qualities. At specific combinations of flow and transition location, a range of critical-flux values was obtained and maximum values were determined. The maximum critical boiling heat flux increased with increasing fluid-flow rate and decreased with increasing length of tube before transition. The variation of the maximum critical flux with flow rate and critical boiling length was similar to that previously obtained with water.

3. Tube-inner-wall temperatures upstream of transition were essentially uniform and were only slightly greater (less than 20° R) than the fluid saturation temperature. Wall temperatures downstream of transition were considerably greater and the wall-temperature profiles generally resembled those obtained in film-boiling studies. The form of the wall-temperature rise downstream of transition appeared to be strongly dependent on the fluid quality at the point of transition. Maximum wall temperatures of 900° and 1800° R were obtained with hydrogen and nitrogen, respectively.

4. Fluctuations of pressure, flow rate, and temperature occurred during some of the boiling tests. Under some conditions, maximum critical-heat-flux values were attained during stable operation with fluctuations. In other cases the fluctuations became uncontrolled, and restabilization of the test condition resulted in critical-flux values less than the maximum values.

5. No measurable pressure drop across the test section was obtained at any condition.

Lewis Research Center

National Aeronautics and Space Administration
Cleveland, Ohio, May 29, 1962

APPENDIX A

COMPUTATIONS AND DATA REDUCTION

Temperature Drop Across Tube Wall

An analysis of the thermal and electric flow in an electrically heated tube is given in references 12 and 13. The basic assumptions of this analysis are negligible radial-voltage gradient and negligible axial-temperature gradient. For the case of a perfectly insulated outer wall, in which the thermal and electrical conductivities of the wall are linear functions of temperature, the equation for the temperature drop across a tube wall may be written as

$$t_{w,o} - t_{w,i} = \frac{JI^2 r_o^2 R_o \left(\frac{R_{av}}{R_o}\right)^2}{k_o A_c^2} \frac{F}{1 + \sqrt{1 - AF}} \quad (A1)$$

where

$$F = \ln\left(\frac{1}{1 - S}\right) - \left(S - \frac{S^2}{2}\right) \quad (A2)$$

$$S = 1 - \frac{r_i}{r_o} \quad (A3)$$

$$\frac{R_{av}}{R_o} = \frac{S - \frac{S^2}{2}}{S - \frac{S^2}{2} + \frac{BS^3}{6}} \quad (A4)$$

$$A = \frac{JI^2 r_o^2 R_o \left(\frac{R_{av}}{R_o}\right)^2}{A_c} \frac{\alpha_o}{k_o} \quad (A5)$$

$$B = \frac{JI^2 r_o^2 R_o \left(\frac{R_{av}}{R_o}\right)^2}{A_c^2} \frac{\beta_o}{k_o} \quad (A6)$$

(All symbols are defined in appendix B.) For the conditions of this investigation,

$$\left(\frac{R_{av}}{R_o}\right)^2 \approx 1$$

Substituting the proper constants and dimensions in equation (A1) gives the tube-wall-temperature drop as

$$t_{w,o} - t_{w,i} = 2465I^2 \frac{R_o}{k_o} \left(\frac{0.0131}{1 + \sqrt{1 - 0.0131 A}} \right) \quad (A7)$$

and

$$A = 2465I^2 \frac{R_o \alpha_o}{k_o} \quad (A8)$$

($R_o = (\text{ohms})(\text{sq ft})/\text{ft}$; $k_o = \text{lb force}/(\text{sec})(^\circ\text{R})$). The heat flux at the tube inner wall is given by

$$q = \frac{JI^2 R_o}{2\pi r_i A_c} \left(\frac{R_{av}}{R_o} \right) \quad (A9)$$

which for this investigation becomes

$$q = 5.22 \times 10^4 R_o I^2 \quad (A10)$$

($R_o = (\text{ohms})(\text{sq ft})/\text{ft}$).

The variation of the thermal conductivity of 303, 304, and 347 stainless steel with temperature is given in figure 18. The variation of the tube electrical resistance with temperature is given in figure 19. The computed tube-wall-temperature drop is given in figure 20 as a function of the heat flux and the tube-outer-wall temperature. For the conditions of the investigation, the wall-temperature drop ranges up to 20°R for the hydrogen conditions and up to 7°R for the nitrogen test conditions. These computed wall-temperature drops should be applied only for readings of thermocouples located in a region of negligible axial-temperature gradient.

Heat Flux

The local heat fluxes tabulated in table II were computed by

$$q = 282I^2R \quad (A11)$$

which is the same as equation (A10) with a change in the constant resulting from using the resistance in ohms per inch of tube. The heat fluxes tabulated in table II include not only the critical heat flux but also the heat flux at the end of the tube, which was essentially constant over the entire tube length for the subcritical flux conditions (no transition).

APPENDIX B

SYMBOLS

A	factor defined in eq. (A5), dimensionless
A_c	tube-wall cross-sectional area, 4.5×10^{-4} sq ft
B	factor defined in eq. (A6), dimensionless
c_p	specific heat of liquid at constant pressure, Btu/(lb mass)(°R)
D	tube inside diameter, 0.04625 ft (0.555 in.)
F	factor defined in eq. (A2), dimensionless
G	test fluid mass velocity, lb mass/(hr)(sq ft)
h_{fg}	heat of vaporization, Btu/lb mass
I	heating current, amp
J	mechanical equivalent of heat, 778.3 ft-lb/Btu or 0.7376 lb force/(w)(sec)
k	thermal conductivity, Btu/(hr)(sq ft)(°R/ft) or lb force/(sec)(°R)
L	distance along tube axis measured from inlet station, in. (total length of tube, $16\frac{1}{8}$ in.)
p	pressure, lb/sq in. abs
Q	rate of heat flow, Btu/hr
q	heat flux, Btu/(hr)(sq ft)
R	tube electrical resistance, (ohms)(sq ft)/ft or ohms/in. of tube
r	radius measured from tube centerline, ft
S	factor defined in eq. (A3), dimensionless
t	temperature, °R
w	fluid mass-flow rate, lb mass/hr
x	fluid quality or mass fraction of vapor defined in eq. (1), dimensionless

- α coefficient of thermal conductivity as function of temperature,
 $1/^{\circ}\text{R}$
- β coefficient of electrical resistivity as function of temperature,
 $1/^{\circ}\text{R}$

Subscripts:

- av arithmetical average
- cr critical (conditions at point of sudden rise of tube-wall temperature)
- ex exit of tube
- i inside surface of tube
- in inlet of tube
- o outside surface of tube
- sat saturation condition
- w wall of tube

REFERENCES

1. Zuber, Novak, and Fried, Erwin: Two-Phase Flow and Boiling Heat Transfer to Cryogenic Liquids. Paper 1709-61, Am. Rocket Soc., Inc., 1961.
2. DeBortoli, R. A., et al.: Forced-Convection Heat Transfer Burnout Studies for Water in Rectangular Channels and Round Tubes at Pressure Above 500 Psia. WAPD-188, Westinghouse Electric Corp., Oct. 1958.
3. Silvestri, Mario: Two-Phase (Steam and Water) Flow and Heat Transfer. Paper 39, 1961 Int. Heat Transfer Conf., Boulder (Colo.), Aug. 28-Sept. 1, 1961.
4. Lowdermilk, Warren H., Lanzo, Chester D., and Siegel, Byron L.: Investigation of Boiling Burnout and Flow Stability for Water Flowing in Tubes. NACA TN 4382, 1958.
5. Forster, K. E., and Greif, R.: Heat Transfer to a Boiling Liquid - Mechanism and Correlations. Jour. Heat Transfer, ser. C, vol. 81, no. 1, Feb. 1959, pp. 43-53.
6. Aladyev, I. T., et al.: Boiling Crisis in Tubes. Paper 28, 1961 Int. Heat Transfer Conf., Boulder (Colo.), Aug. 28-Sept. 1, 1961.
7. Wright, C. C., and Walters, H. H.: Single Tube Heat Transfer Tests, Gaseous and Liquid Hydrogen. TR 59-423, WADC, Aug. 1959.
8. Hendricks, R. C., Graham, R. W., Hsu, Y. Y., and Friedman, R.: Experimental Heat Transfer and Pressure Drop of Liquid Hydrogen Flowing Through a Heated Tube. NASA TN D-765, 1961.
9. Scott, Russell B.: Cryogenic Engineering. D. Van Nostrand Co., Inc., 1959.
10. Johnson, Victor J.: A Compendium of the Properties of Materials at Low Temperature (Phase 1). Pt. 1. Properties of Fluids. TR 60-56, WADD, July 1960.
11. Chang, Yan-Po, and Snyder, Nathan W.: Heat Transfer in Saturated Boiling. Preprint 104, ASME-AIChE, 1959.
12. Powell, Walter B.: Heat Transfer to Fluids in the Region of the Critical Temperature. Prog. Rep. 20-285, Jet Prop. Lab., C.I.T., Apr. 1, 1956.

13. Kreith, F., and Summerfield, M.: Investigation of Heat Transfer at High Heat-Flux Densities: Experimental Study with Water of Friction Drop and Forced Convection with and without Surface Boiling in Tubes. Prog. Rep. 4-68, Jet Prop. Lab., C.I.T., Apr. 2, 1948.
14. Zimmerman, James E.: Heat Conduction in Alloys and Semi-Conductors at Low Temperatures. D.Sc. Thesis, Carnegie Inst. Tech., 1951.

TABLE I. - THERMOCOUPLE LOCATIONS

Description	Station	Distance from inlet (measured positively downstream), in., for -	
		Runs 100 to 220	Runs 220 to 327
Tube outer wall	1	0.5	0.52
	2	1.5	1.5
	3	2.5	2.5
	4	3.5	3.41
	5	4.5	4.5
	6	5.5	5.41
	7	6.5	6.45
	8	7.5	7.53
	9	8.5	8.53
	10	9.5	9.53
	11	10.5	10.5
	12	11.5	11.48
	13	----	14.06
	14	----	14.56
	15	15.6	15.61
Copper bus			
Far	16	$-1\frac{7}{8}$	-1.81
Near	17	$-7/8$	-.88
Inlet section			
Near	18	$-1/2$	-0.5
Far	19	$-1\frac{1}{2}$	-1.44
Outlet section	20	17	17.22

[illegible]

Heat flux, length-to-diameter ratio, and quality are subcritical values and are taken as of tube-exit conditions.

TABLE II. - Concluded.

(a) Concluded. Hydrogen

Run	Pressure, lb./sq. in.	Saturation temperature, °F.	Fluid inlet temperature, °F.	Fluid exit temperature, °F.	Inlet mass flow, lb./hr.	Exit super- heat, °F.	Mass velocity, lb./sq. ft.	Heater current, amp.	Critical heat flux, Btu (hr)(sq. ft.)	Critical boiling length- to- diameter ratio	Critical quality	Tube outer-wall					
												1	2	3	4	5	6
213	11.0	48.4	42.3	41.4	3.4	-0.2	4,720	263	6,200	21.7	0.77	33	73	10	14	12	
214	11.0	48.6	42.4	41.3	3.7	-1.2	4,700	266	6,300	20.0	.76	42	77	30	29	54	12
215	11.0	48.6	42.4	41.1	3.0	-1.3	4,380	272	6,700	24.1	.61	42	77	10	42	54	52
216	11.0	48.7	43.1	40.3	3.7	-1.3	4,400	313	8,800	20.0	.70	42	80	12	42	58	14
217	11.0	48.7	43.1	40.3	1.7	-1.4	4,300	---	---	---	---	33	70	48	41	41	42
218	11.0	50.4	50.4	50.4	0	0	0	---	---	---	---	33	70	36	36	36	33
219	11.0	48.4	43.2	42.3	2.2	---	4,100	291	7,700	21.0	.62	4	52	34	42	58	54
220	11.0	48.5	42.1	41.7	2.9	-1.4	4,170	312	8,800	20.0	.70	36	74	10	41	54	12
221	11.0	48.6	42.4	42.6	3.0	-0.6	4,350	---	---	---	---	42	70	47	42	47	41
222	11.0	48.4	43.4	41.1	2.0	-1.1	4,030	316	9,000	19.0	.76	42	80	12	30	58	16
223	11.0	48.2	43.5	40.7	1.7	-1.3	4,470	301	11,100	17.2	.60	41	81	14	68	60	18
224	11.0	48.4	43.1	44.0	1.4	-1.3	6,770	317	9,100	20.0	.70	10	88	16	18	62	16
225	11.0	48.6	43.6	44.0	1.4	-1.1	6,820	316	9,000	20.2	.79	10	88	16	18	64	60
226	11.4	48.1	43.7	42.8	1.4	-1.1	6,780	312	8,800	20.2	.76	10	89	16	18	62	60
227	11.4	48.1	43.7	44.8	1.0	-1.1	6,720	363	11,900	20.2	.61	10	90	16	18	68	62
228	11.5	48.6	43.0	43.7	2.8	-1.3	4,440	253	6,300	26.2	.82	48	60	54	47	60	56
229	11.5	48.7	43.1	43.6	2.6	-1.1	10,630	387	13,600	26.2	.73	48	61	60	18	68	64
230	11.5	48.1	43.1	43.4	2.4	-1.1	12,620	416	15,700	26.2	.71	48	66	60	12	68	64
231	11.5	48.1	43.4	41.4	2.1	-1.1	16,300	458	19,150	26.2	.60	48	66	64	10	74	70
232	11.0	48.4	43.6	---	1.8	---	7,990	433	17,150	12.0	.60	48	63	66	64	71	74
233	11.0	48.1	43.1	---	2.0	---	7,990	424	16,400	7.2	.30	70	70	72	72	380	443
234	11.0	48.4	43.6	---	1.8	0	5,740	373	12,600	19.2	.89	48	63	56	42	66	62
235	11.0	48.4	43.5	45.9	2.1	-1.5	3,820	382	13,200	11.7	.63	48	62	58	56	66	64
236	11.0	48.5	43.2	46.2	2.3	-1.7	6,000	389	13,750	14.0	.69	50	63	56	58	68	66
237	11.0	48.2	43.3	48.9	1.9	-1.7	9,530	440	17,650	13.5	.63	50	60	62	62	74	72
238	11.0	48.7	42.5	43.7	3.4	0	13,380	443	17,850	7.5	.17	45	79	62	54	263	390
239	11.0	48.9	44.2	48.0	1.0	-1.1	12,660	470	20,000	15.0	.53	47	93	62	---	74	72
240	11.0	48.6	41.2	45.5	4.4	-1.1	16,200	415	15,650	5.0	.04	48	71	60	327	389	393
241	11.0	48.1	41.7	45.5	3.8	0	16,000	424	16,300	10.0	.17	47	75	60	54	66	100
242	11.0	48.5	41.7	45.0	3.9	-1.1	16,860	425	16,350	12.5	.22	47	73	60	54	68	60
243	11.0	48.7	42.0	46.0	2.9	-1.5	11,200	444	17,900	13.5	.45	47	68	58	58	60	60
244	11.0	48.6	43.5	44.0	2.3	106.2	3,320	378	12,950	8.7	.64	42	75	52	52	58	277
245	11.0	48.6	43.8	45.6	1.9	0	6,190	397	14,300	8.5	.42	42	77	52	52	58	281
246	11.0	48.7	43.6	46.0	2.1	-1.3	9,310	419	15,900	8.5	.30	39	75	52	45	62	296
247	11.0	48.7	44.6	45.9	1.1	-1.1	10,920	430	16,750	8.5	.25	39	80	52	36	64	276
248	11.0	48.2	44.6	45.4	.6	-1.2	11,850	447	16,150	8.8	.29	36	79	54	47	70	282
249	11.0	48.7	45.6	---	1.1	---	8,700	449	18,150	2.5	.12	45	97	268	305	374	459
250	11.0	48.4	45.5	45.5	-1.1	-1.1	10,690	---	---	---	---	45	80	50	47	47	45
251	11.0	48.6	44.2	45.7	1.6	-1.1	14,670	476	20,500	18.2	.46	42	75	58	52	66	64

(b) Nitrogen

254	11.5	163.2	162.0	165.0	1.2	1.8	17,030	297	8,870	21.5	0.57	165	198	170	175	173	171
255	11.5	162.8	163.0	164.0	4.8	1.2	24,030	304	9,250	25.0	.46	163	195	169	171	172	171
256	11.5	163.0	160.0	165.0	3.0	2.0	24,500	322	10,400	23.7	.50	164	197	170	179	174	172
257	11.5	161.4	163.0	161.0	3.4	-1.4	36,000	345	11,900	25.0	.38	162	195	169	167	171	171
258	11.5	160.7	167.5	160.5	3.2	-1.2	30,400	323	10,400	23.5	.39	160	194	167	171	170	170
259	11.5	163.0	160.0	163.0	3.0	0	29,800	313	9,800	21.5	.35	163	197	170	174	173	172
260	11.5	163.5	161.5	163.5	2.0	0	42,300	355	12,600	24.2	.36	165	197	170	165	175	173
261	11.5	161.4	167.0	162.0	4.4	-1.6	31,000	325	10,600	24.0	.39	161	193	167	171	171	170
262	11.5	161.2	167.0	162.0	4.2	-1.8	30,900	326	10,650	23.9	.43	161	193	168	173	171	170
263	11.5	161.3	167.0	160.5	4.3	-1.8	28,700	309	9,550	22.9	.47	163	195	167	169	170	169
264	11.5	161.2	168.0	160.5	3.2	-1.7	15,100	314	8,850	22.0	.49	161	194	165	168	169	168
265	11.5	163.2	167.5	163.0	5.7	-1.2	19,750	301	9,050	22.0	.48	162	194	167	163	171	170
266	11.5	161.4	168.0	160.5	3.4	-1.9	16,250	316	10,000	22.0	.49	163	195	167	165	171	170
267	11.5	162.2	169.0	162.0	3.2	-1.2	22,850	302	9,150	22.5	.44	164	196	169	167	172	171
268	11.5	162.0	169.0	162.0	3.0	0	27,200	316	10,000	24.0	.43	164	197	168	175	171	170
269	11.5	161.3	167.0	161.0	4.3	-1.3	25,100	352	12,350	22.0	.47	159	194	168	171	170	168
270	11.5	161.3	167.0	162.0	4.3	-1.7	24,400	367	13,500	22.0	.78	163	194	165	175	170	169
271	11.5	161.4	167.0	161.0	4.4	-1.4	24,100	361	13,000	22.0	.47	159	194	166	165	171	170
272	11.5	161.5	167.5	161.0	4.0	-1.5	23,600	371	13,800	22.0	.44	160	195	165	165	171	170
273	11.5	161.4	168.0	162.0	3.4	-1.6	24,500	308	8,500	23.5	.44	160	191	165	167	168	167
274	11.5	161.7	167.0	161.5	4.2	-1.2	31,100	408	16,700	22.0	.47	160	187	167	171	172	171
275	11.5	163.0	169.0	163.0	4.0	0	31,000	400	16,000	23.0	.73	160	198	169	171	173	172
276	11.5	163.2	169.0	163.0	4.2	-1.2	31,000	406	16,800	23.0	.75	161	200	170	178	174	173
277	11.5	163.2	169.0	163.0	4.2	-1.2	31,200	413	17,100	22.9	.47	160	200	170	166	173	172
278	11.5	161.4	167.0	160.0	4.4	-1.4	43,300	453	20,550	22.0	.47	160	201	170	178	175	172
279	11.5	161.4	166.5	160.5	4.9	-1.9	40,600	453	20,550	22.0	.72	161	202	170	168	174	173
280	11.5	160.6	167.0	161.0	3.8	-1.2	42,700	346	11,950	24.0	.40	160	194	167	171	171	170
281	11.5	161.5	168.0	161.0	3.5	-1.5	36,300	489	24,000	22.0	.61	161	205	171	172	177	176
282	11.5	161.2	167.0	161.0	4.2	-1.2	32,400	154	42,550	22.0	.08	159	187	162	167	163	162
283	11.5	161.1	167.0	161.0	4.1	-1.1	31,400	208	9,400	22.0	.18	160	188	163	167	164	163
284	11.5	161.1	167.0	161.0	4.1	-1.1	31,200	255	9,500	22.0	.28	160	189	163	169	167	164
285	11.5	161.1	167.0	161.0	4.1	-1.1	31,700	323	10,400	22.0	.46	160	192	165	170	168	167
286	11.5	160.6	168.5	168.7	1.7	-1.5	31,900	---	---	---	---	160	184	169	163	160	160
287	11.5	161.3	169.0	161.0	2.3	-1.3	26,000	325	10,550	17.0	.51	161	197	166	166	171	167
288	11.5	161.8	169.7	162.0	2.1	-1.2	24,400	384	14,700	3.0	.08	164	294	833	1132	1320	1455
289	11.5	161.2	168.2	---	---	---	30,600	410	17,000	28.0	.80	---	---	---	---	---	---
290	11.5	161.2	168.2	---	---	---	37,500	435	21,300	28.0	.80	---	---	---	---	---	---
291	11.5	161.4	166.0	161.4	3.4	0	15,500	315	10,000	29.0	.93	---	---	---	---	---	---
292	11.5	161.7	166.0	162.0	3.7	0	53,800	503	26,600	29.0	.69	---	---	---	---	---	---
293	11.5	161.5	166.5	161.4	3.0	0	24,000	367	13,500	29.0	.73	---	---	---	---	---	---
294	11.5	161.0	169.0	161.0	2.0	0	30,400	390	15,500	29.0	.82	---	---	---	---	---	---

EXPERIMENTAL DATA

(a) Concluded. Hydrogen

temperature, °R, at station -														Copper bus temperature, °R		Inlet plenum wall temperature, °R		Exit plenum wall temperature, °R		Amplitude of tube wall temperature fluctuations		Remarks
7	8	9	10	11	12	13	14	15	16	17	18	19	20	Far	Near	Near	Far	Near	Far	±0R	At station	
50	50	50	54	58	62	65	100	171	272	318	32	52	54	50	56	52	54	50	56	13	13	Transition; maximum-critical-flux value
52	52	52	56	58	62	62	80	122	274	318	54	54	54	50	56	52	54	50	56	14	14	
52	52	52	56	58	62	62	109	119	274	318	54	54	54	50	56	52	54	50	56	15	15	
52	54	54	56	58	62	62	379	379	392	375	280	320	294	242	163	14	12	14	12	14	12	No-heat run; control valves in same position as in run 268 Vented system to atmosphere
42	42	42	504	47	42	33	33	42	265	307	42	42	42	42	42	42	42	42	42	42	42	
33	33	33	505	36	33	29	31	33	262	306	33	29	30	249	192	148	2	14	2	14	2	
52	52	52	56	58	62	62	415	597	281	326	315	268	285	40	40	40	40	40	40	40	40	Transition; maximum-critical-flux value
52	52	52	56	58	62	62	415	597	281	326	315	268	285	40	40	40	40	40	40	40	40	
52	52	52	56	58	62	62	415	597	281	326	315	268	285	40	40	40	40	40	40	40	40	
54	56	56	56	103	260	429	437	421	297	355	346	306	211	23	11	23	11	23	11	23	11	Transition; maximum-critical-flux value Transition; maximum-critical-flux value; difficult to stabilize because of flow oscillations
56	56	109	549	369	443	592	605	164	293	359	489	426	212	21	0	21	0	21	0	21	0	
56	56	56	60	60	60	124	235	186	287	352	62	60	60	42	13	17	14	13	17	14	13	
58	58	58	62	62	62	61	167	189	287	351	62	60	60	20	13	20	13	20	13	20	13	Transition; maximum-critical-flux value
58	58	58	62	62	62	62	66	150	287	352	62	60	60	60	60	60	60	60	60	60	60	
60	60	60	62	62	62	64	70	230	294	358	66	64	64	64	64	64	64	64	64	64	64	
58	54	54	56	60	60	60	83	105	283	327	60	58	60	17	14	17	14	17	14	17	14	Transition; maximum-critical-flux value
62	62	62	64	64	64	64	72	108	296	345	68	66	64	34	10	34	10	34	10	34	10	
64	62	64	64	64	64	70	72	234	301	347	70	68	68	10	10	10	10	10	10	10	10	
68	68	68	68	72	72	74	60	205	307	354	74	72	100	6	10	6	10	6	10	6	10	Transition; conditions impossible to stabilize; temperatures kept changing
75	561	423	461	492	108	568	571	530	303	350	129	119	270	---	---	---	---	---	---	---	---	
451	467	466	470	490	489	511	312	492	302	349	490	489	341	---	---	---	---	---	---	---	---	
60	60	60	62	260	344	111	522	498	295	345	430	401	245	---	---	---	---	---	---	---	---	Transition; maximum-critical-flux value
60	62	62	254	375	426	566	576	144	297	344	492	460	298	---	---	---	---	---	---	---	---	
64	64	368	379	420	451	524	554	521	298	340	491	469	260	---	---	---	---	---	---	---	---	
72	132	347	439	471	492	555	564	536	307	354	121	114	269	---	---	---	---	---	---	---	---	Transition; maximum-critical-flux value
424	416	406	401	409	410	424	429	409	303	359	451	435	297	---	---	---	---	---	---	---	---	
58	68	239	375	423	434	504	511	497	314	361	480	458	251	---	---	---	---	---	---	---	---	
373	361	357	351	353	349	347	352	332	300	350	515	510	140	---	---	---	---	---	---	---	---	Transition
365	380	375	372	370	368	362	368	348	301	347	358	353	148	---	---	---	---	---	---	---	---	
58	326	351	354	361	361	361	362	348	300	346	357	352	145	---	---	---	---	---	---	---	---	
451	467	466	470	490	489	511	312	492	302	349	490	489	341	---	---	---	---	---	---	---	---	Transition; maximum-critical-flux value
360	401	447	497	503	514	568	565	530	294	340	609	583	329	---	---	---	---	---	---	---	---	
360	366	415	450	451	465	517	520	435	290	342	497	478	260	---	---	---	---	---	---	---	---	
377	392	404	409	418	421	444	447	424	299	346	497	478	212	---	---	---	---	---	---	---	---	Transition
360	393	406	412	418	420	441	444	419	300	348	495	478	204	13	4	13	4	13	4	13	4	
392	422	434	435	441	442	459	463	430	303	350	451	450	197	---	---	---	---	---	---	---	---	Transition; took 3 hr to obtain equilibrium; at first had increasing temperature profile; later profile peaked
365	618	626	596	576	561	573	577	540	313	364	511	561	270	4	12	4	12	4	12	4	12	
46	46	46	46	50	46	42	42	46	276	301	47	47	46	---	---	---	---	---	---	---	---	No-heat run to check wall thermocouples Transition; similar behavior as in run 522
54	54	101	473	420	441	479	482	415	303	357	462	454	215	---	---	---	---	---	---	---	---	

(b) Nitrogen

171	173	172	173	178	173	865	890	850	348	384	549	179	175	---	---	---	---	---	---	---	---	Transition; on all these runs either power was decreased or flow rate increased as desired transition condition was approached to prevent overheating and instability
171	172	171	172	175	173	451	618	594	348	380	170	174	174	3	15	3	15	3	15	3	15	
172	173	172	173	176	174	705	785	636	348	393	173	175	175	5	16	5	16	5	16	5	16	
171	172	171	171	174	172	552	725	629	345	393	173	173	173	2	16	2	16	2	16	2	16	No transition; close to maximum-critical-flux value
170	170	170	170	173	171	605	650	680	341	377	173	171	171	4	13	4	13	4	13	4	13	
172	174	173	175	179	176	605	630	626	340	376	---	179	175	---	---	---	---	---	---	---	---	
173	174	173	174	177	178	675	900	660	346	363	175	175	173	5	16	5	16	5	16	5	16	No transition; close to maximum-critical-flux value
170	171	170	171	173	171	725	905	639	357	373	173	173	172	---	---	---	---	---	---	---	---	
170	171	170	171	173	171	173	172	172	356	371	172	171	171	---	---	---	---	---	---	---	---	
169	170	170	170	171	171	172	172	172	345	390	171	171	170	---	---	---	---	---	---	---	---	No transition; close to maximum-critical-flux value
168	169	168	168	170	169	171	170	170	343	390	170	170	168	---	---	---	---	---	---	---	---	
170	171	170	171	174	172	760	785	590	340	377	174	173	172	---	---	---	---	---	---	---	---	
170	170	170	170	172	171	723	173	172	345	352	171	171	170	---	---	---	---	---	---	---	---	Transition
171	171	171	171	175	172	781	801	643	343	350	171	173	172	3	16	3	16	3	16	3	16	
170	171	170	171	173	172	680	761	619	348	393	174	173	172	2	16	2	16	2	16	2	16	
168	169	168	169	171	170	171	171	171	342	379	171	171	170	---	---	---	---	---	---	---	---	No transition; maximum-critical-flux value
168	169	168	169	171	170	805	961	736	343	380	171	171	170	12	15	12	15	12	15	12	15	
169	169	169	169	171	170	171	171	171	343	380	171	171	170	11	14	11	14	11	14	11	14	
169	169	169	169	170	171	170	171	171	344	361	171	171	170	---	---	---	---	---	---	---	---	No transition; maximum-critical-flux value
169	170	169	170	171	170	172	172	172	346	363	171	172	170	---	---	---	---	---	---	---	---	
167	168	167	168	170	169	660	736	598	357	373	170	170	169	1	16	1	16	1	16	1	16	
170	171	171	171	172	171	173	174	172	351	390	172	172	171	---	---	---	---	---	---	---	---	No transition; close to maximum-critical-flux value
171	172	171	172	175	173	175	176	174	350	390	173	173	172	---	---	---	---	---	---	---	---	
172	173	172	173	175	174	175	176	175	352	391	174	174	171	---	---	---	---	---	---	---	---	
171	172	172	173	174	173	175	176	174	353	392	174	174	171	3	4	3	4	3	4	3	4	No transition; close to maximum-critical-flux value
171	172	171	172	175	173	175	176	174	361	392	174	174	171	---	---	---	---	---	---	---	---	
172	173	172	173	176	174	175	177	175	362	404	174	174	171	---	---	---	---	---	---	---	---	
169	170	169	170	172	171	690	793	642	343	391	173	172	172	4	16	4	16	4	16	4	16	No transition; close to maximum-critical-flux value
174	175	174	175	179	176	177	179	175	369	411	176	173	171	---	---	---	---	---	---	---	---	
163	163	163	163	164	163	164	164	165	376	361	163	163	166	---	---	---	---	---	---	---	---	
164	164	163	164	165	164	165	166	167	326	365	168	165	167	---	---	---	---	---	---	---	---	No transition
163	166	162	167	169	167	169	163	169	333	470	167	167	168	---	---	---	---	---	---	---	---	
167	166	167	169	170	169	171	171	170	342	360	170	170	167	---	---	---	---	---	---	---	---	
167	166	167	169	170	169	171	171	170	342	360	170	170	167	---	---	---	---	---	---	---	---	No heat pump; thermocouple check
160	166	166	166	167	166	167	166	169	316	356	160	160	160	---	---	---	---	---	---	---	---	
168	169	166	166	166	166	166	166	166	349	385	168	168	168	3	10	3	10	3	10	3	10	
163	163	163	163	164	163	164	164	165	376	361	163	163	166	---	---	---	---	---	---	---	---	Transition; difficult to control
163	163	163	163	164	163	164	164	165	376	361	163	163	166	---	---	---	---	---	---	---	---	
163	163	163	163	164	163	164	164	165	376	361	163	163	166	---	---	---	---	---	---	---	---	
163	163	163	163	164	163	164	164	165	376	361	163	163	166	---	---	---	---	---	---	---	---	All these data taken while attempting to obtain maximum critical flux for transition at end of test; data represent last readings taken before flow power or flow adjustment which caused instability and gave transition equipment at heat flux values considered to be less than maximum critical flux
163	163	163	163	164	163	164	164	165	376	361	163	163	166	---	---	---	---	---	---	---	---	
163	163	163	163	164	163	164	164	165	376	361	163	163	166	---	---	---	---	---	---	---	---	

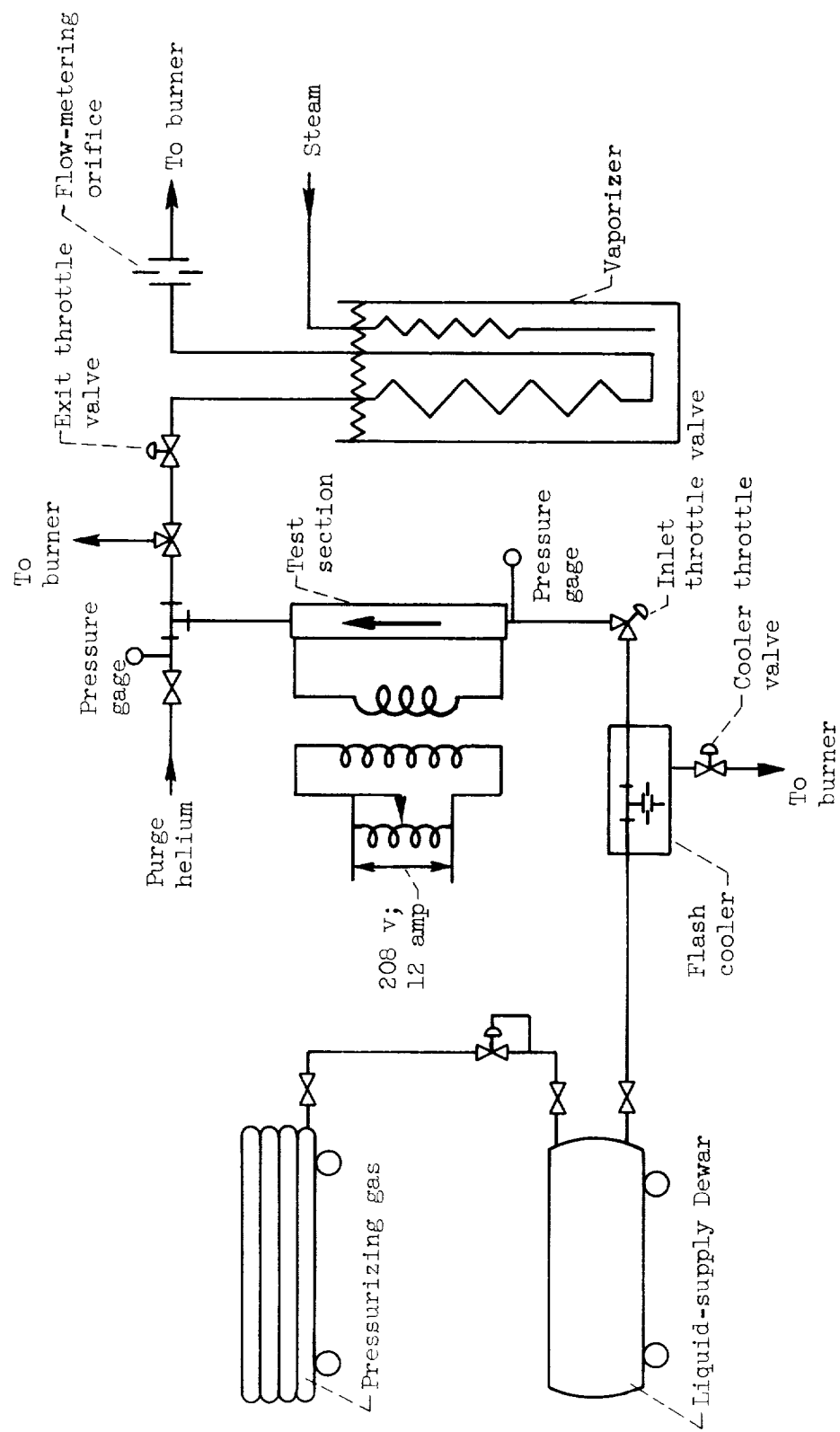


Figure 1. - Schematic drawing of cryogenic boiling-heat-transfer apparatus.

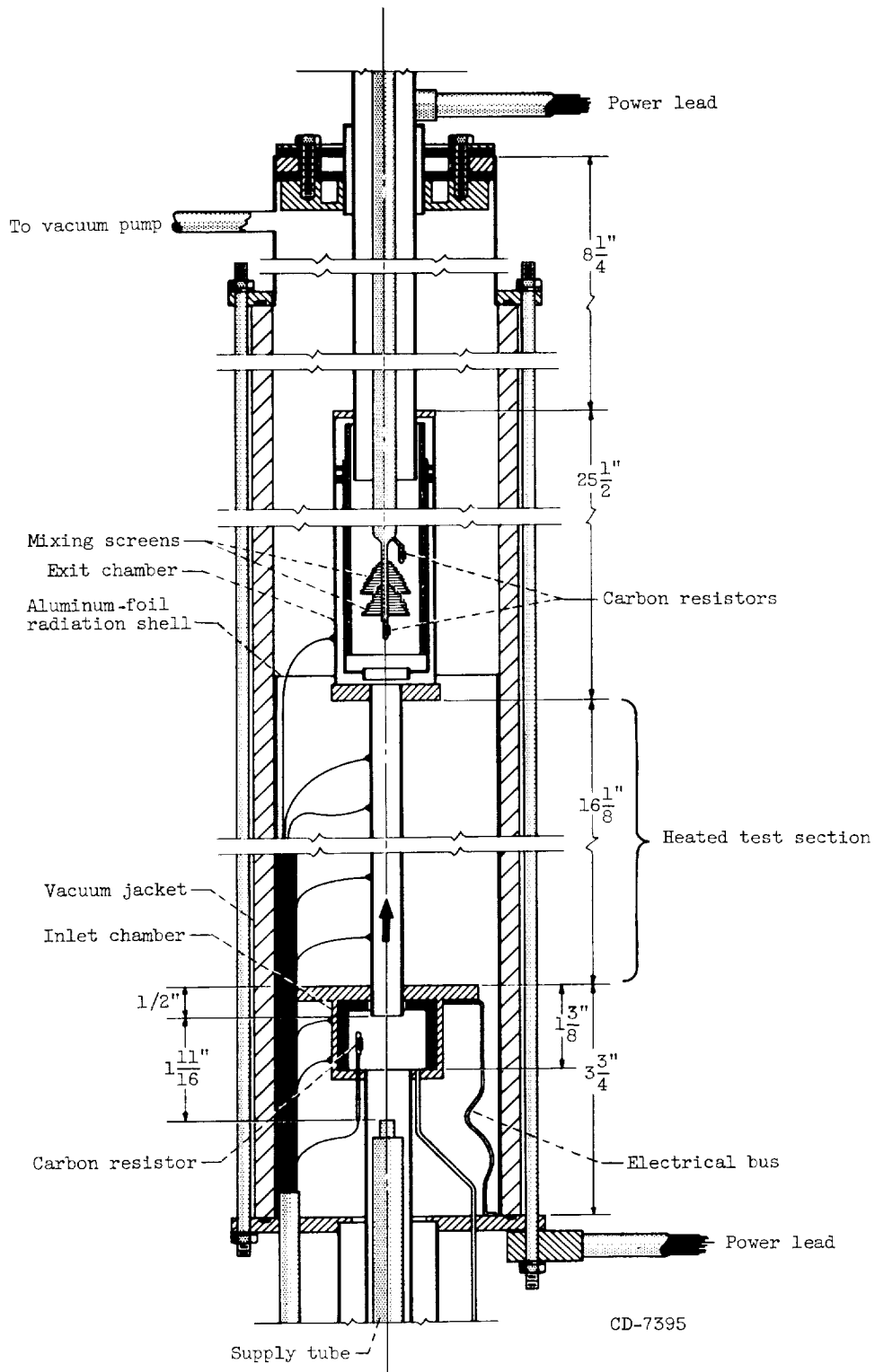
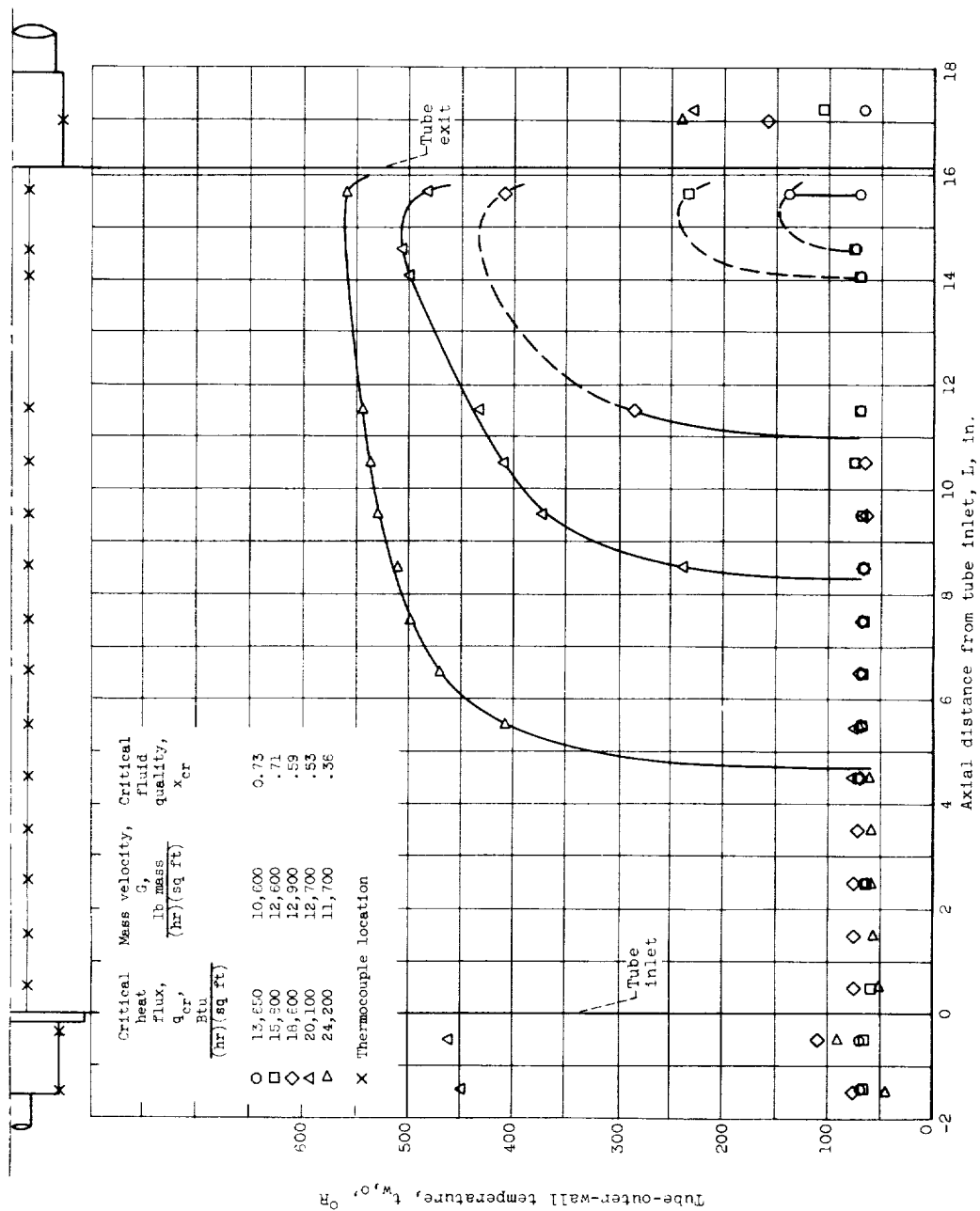
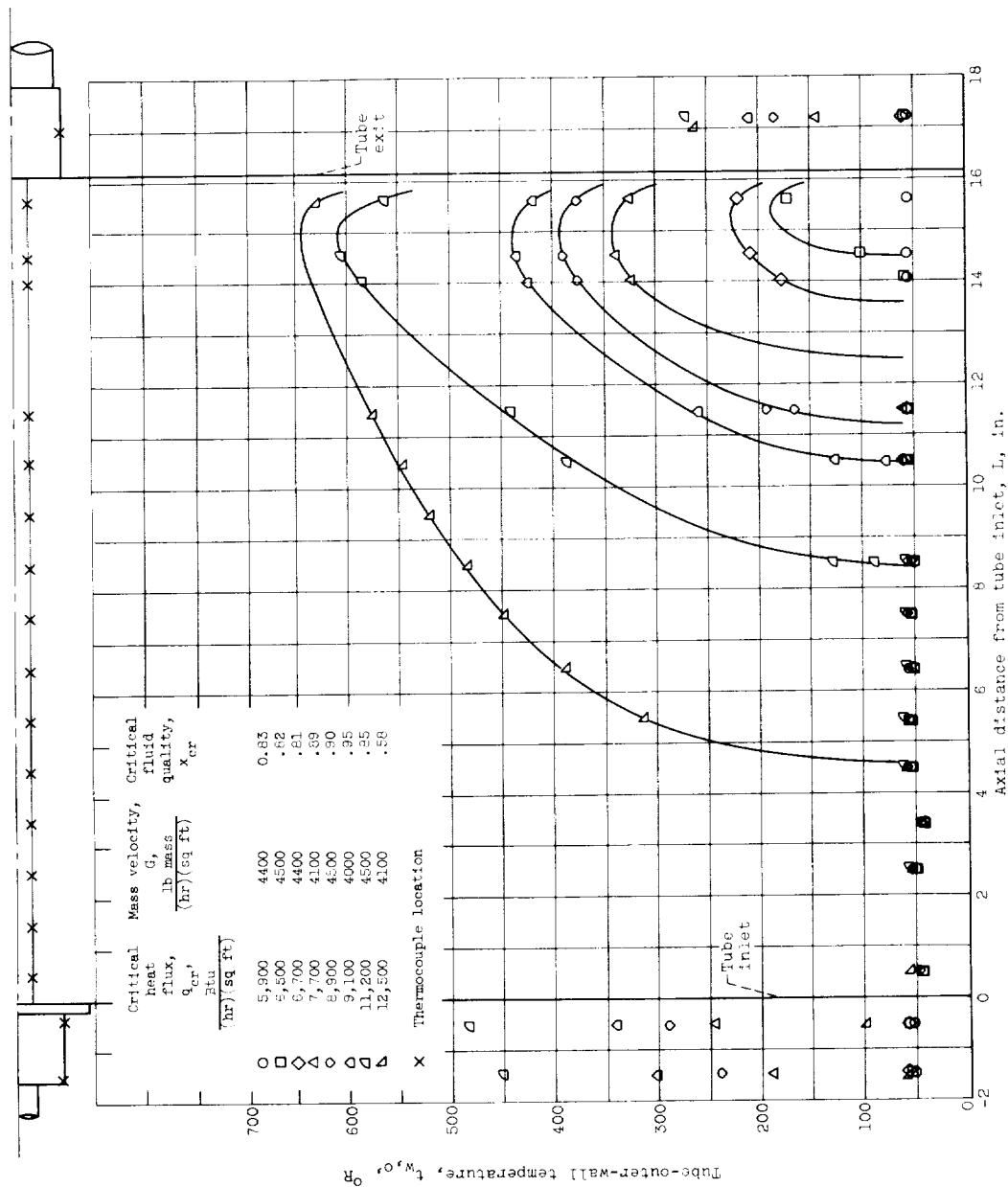


Figure 2. - Details of test section, inlet, and exit.



(a) Mass velocity, approximately 12,000 pounds per hour per square foot.

Figure 3. - Tube-outer-wall temperature profiles for constant mass velocity and varying heat flux and location of transition. Liquid hydrogen; test-section pressure, approximately 30 pounds per square inch absolute; average inlet subcooling, 20 °F.



(b) Mass velocity, approximately 4500 pounds per hour per square foot.

Figure 3. - Concluded. Tube-outer-wall temperature profiles for constant mass velocity and varying heat flux and location of transition. Liquid hydrogen; test-section pressure, approximately 50 pounds per square inch absolute; average inlet subcooling, 26 R.

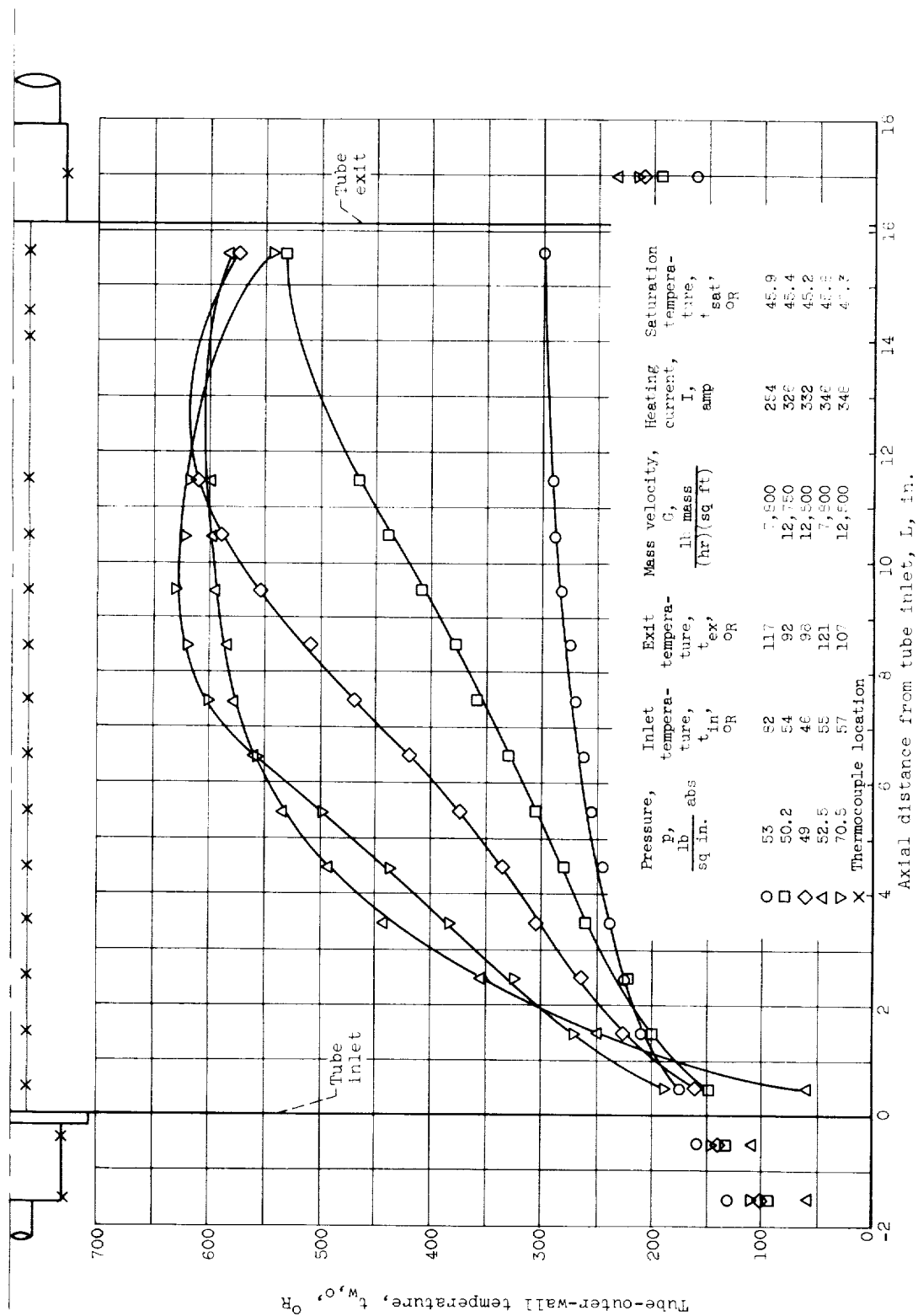
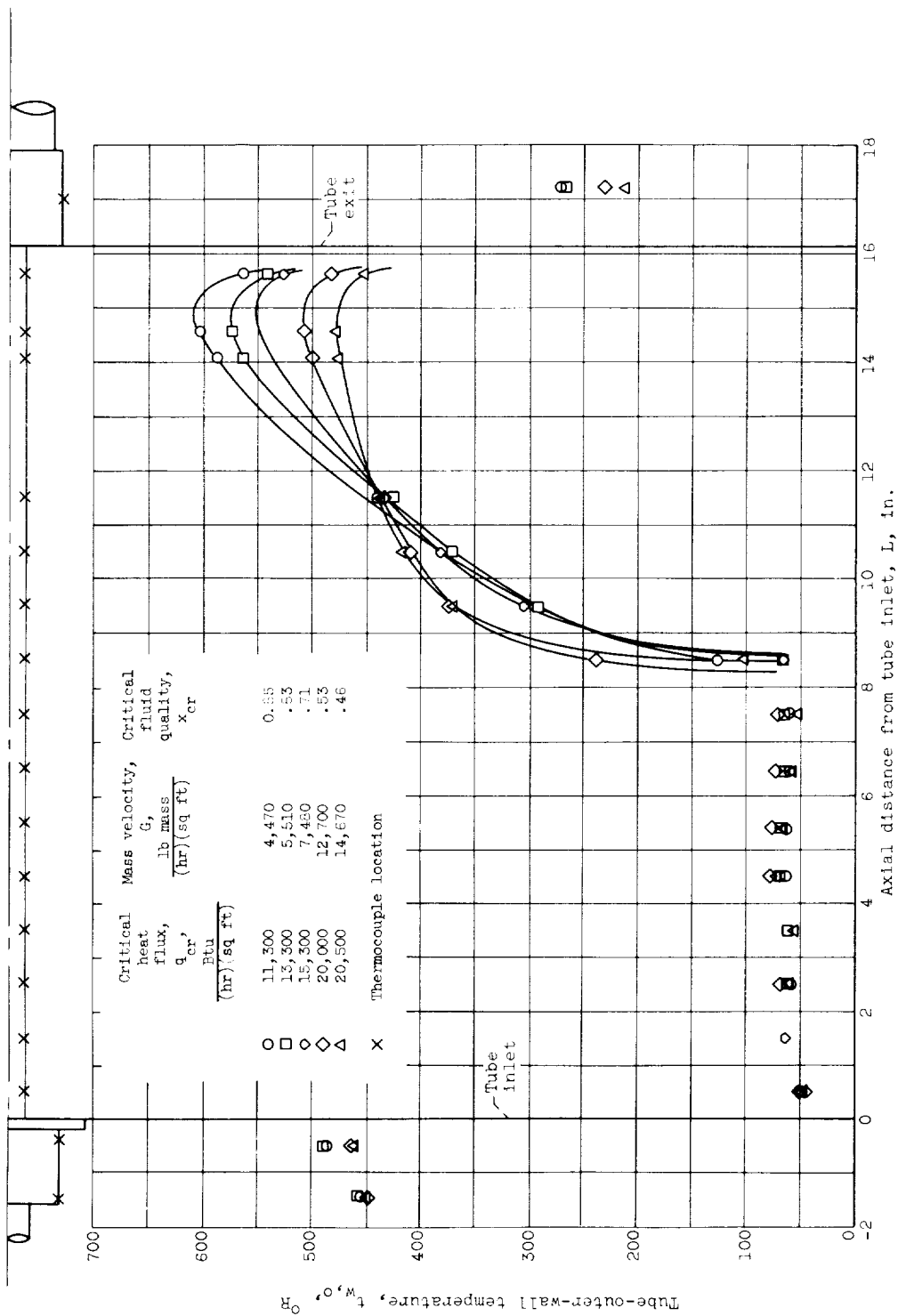
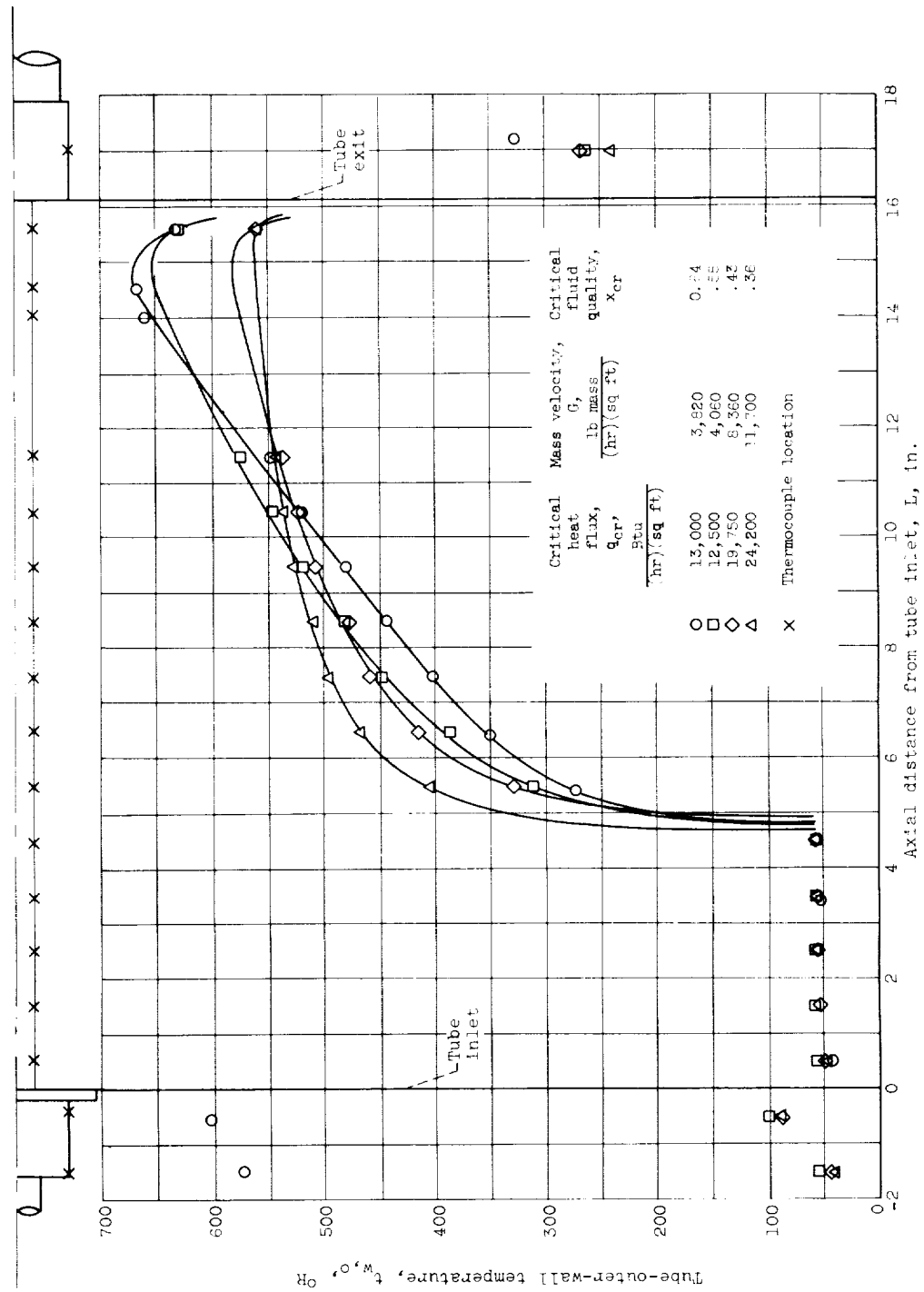


Figure 4. - Tube-outer-wall temperature profiles for flow of cool hydrogen gas through heated tube at several pressure, temperature, flow-rate, and heating-rate conditions.



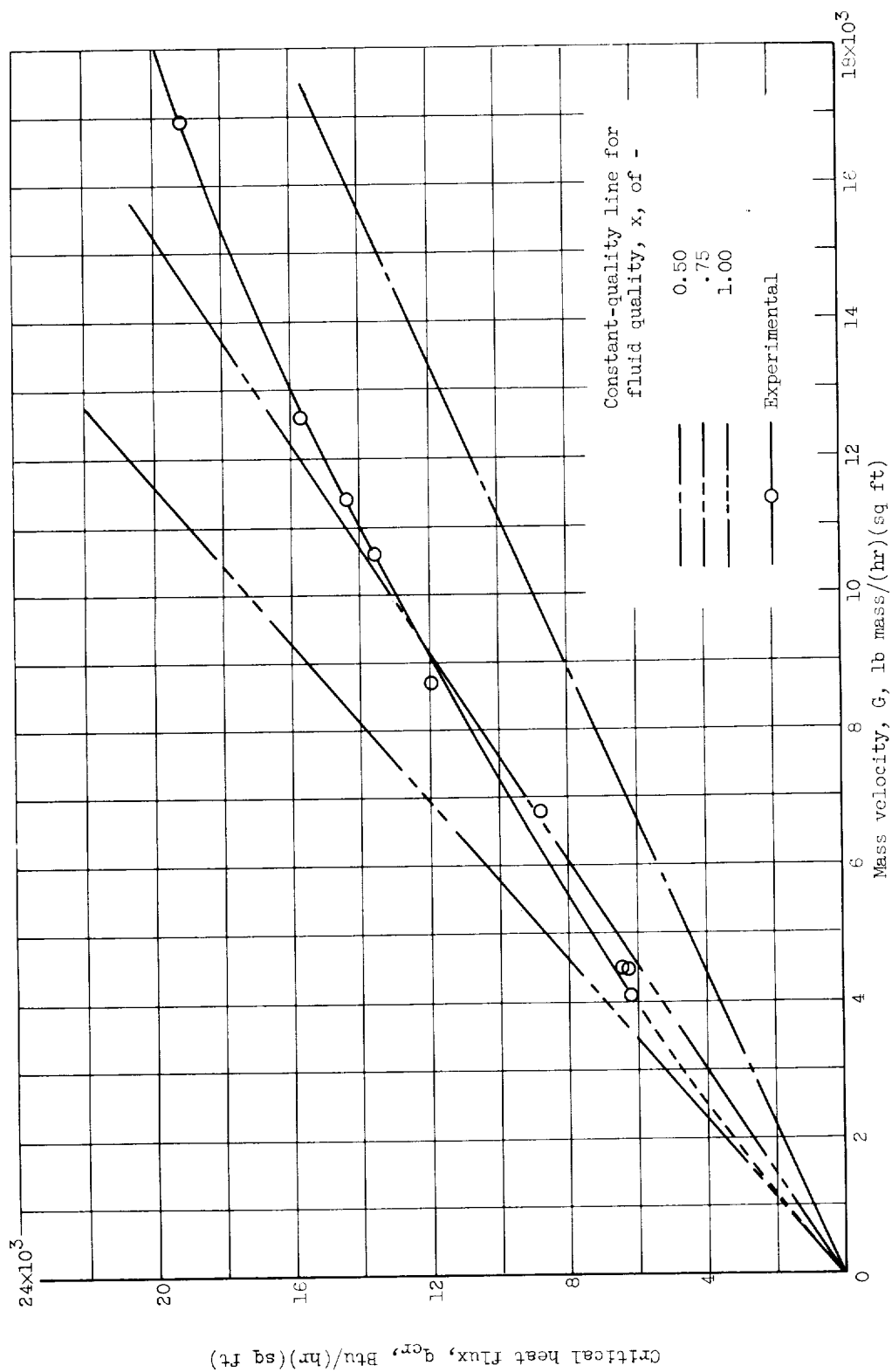
(a) Critical-boiling-length-to-diameter ratio, approximately 15.

Figure 5. - Tube-outer-wall temperature profiles for constant transition location and varying heat flux and mass velocity. Liquid hydrogen; test-section pressure, approximately 50 pounds per square inch absolute; average inlet subcooling, 2° R.



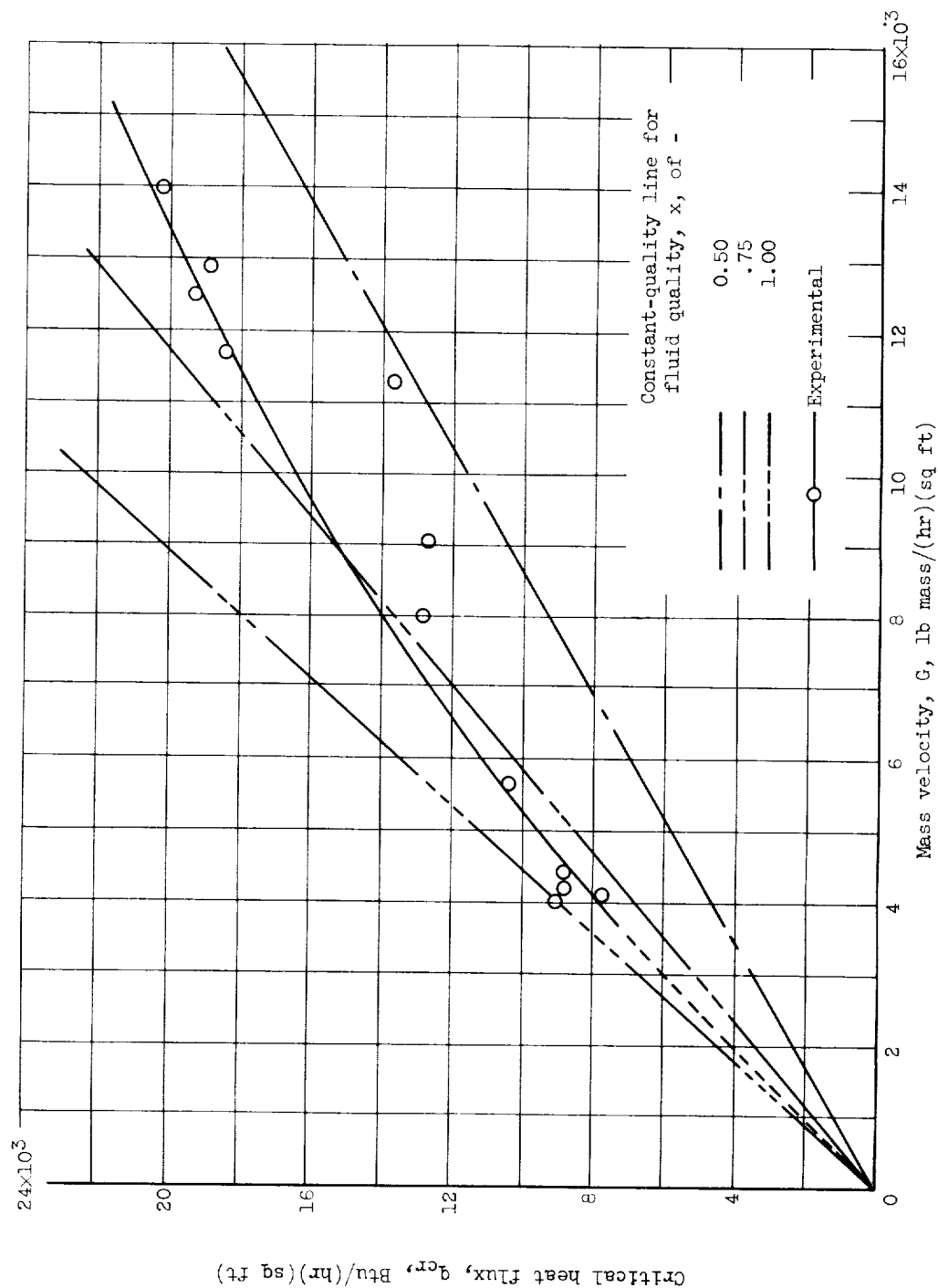
(b) Critical-boiling-length-to-diameter ratio, approximately 5.5.

Figure 5. - Concluded. Tube-outer-wall temperature profiles for constant transition location and varying heat flux and mass velocity. Liquid hydrogen; test-section pressure, approximately 50 pounds per square inch absolute; average inlet subcooling, 20 R.



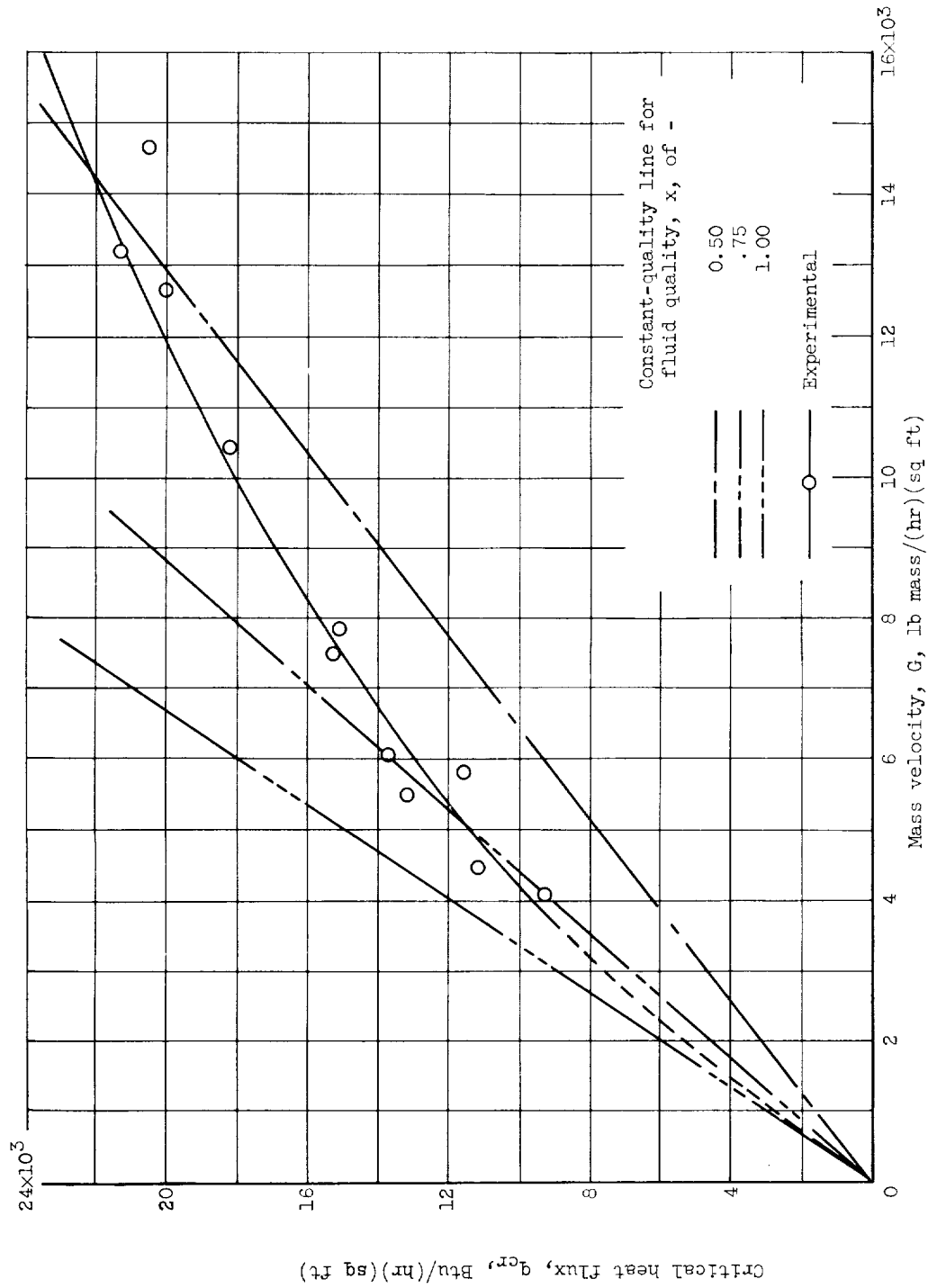
(a) Critical-boiling-length-to-diameter ratio, approximately 26.

Figure 6. - Variation of critical heat flux with mass velocity. Liquid hydrogen; test-section pressure, approximately 50 pounds per square inch absolute; average inlet subcooling, 20° R.



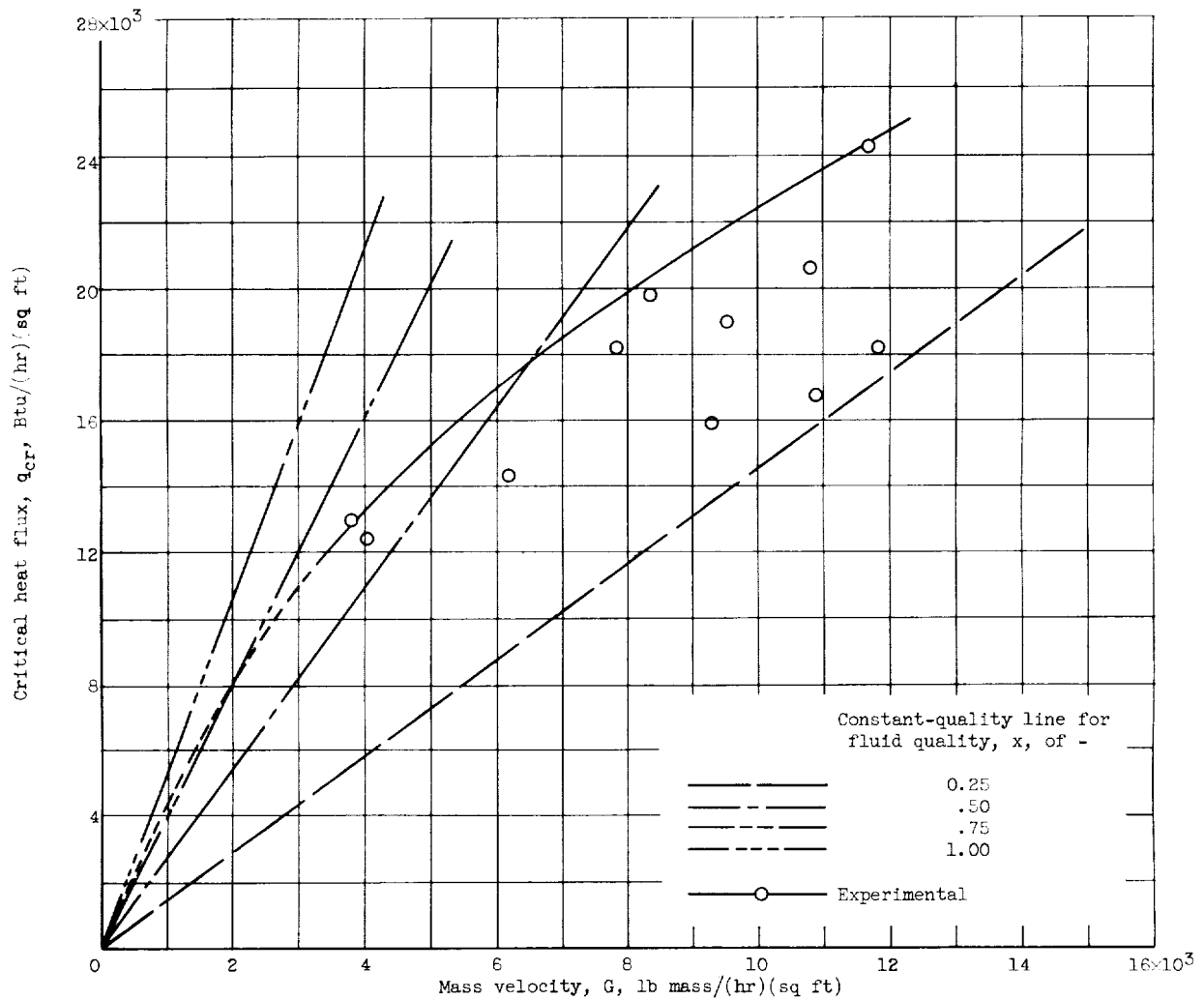
(b) Critical-boiling-length-to-diameter ratio, approximately 20.

Figure 6. - Continued. Variation of critical heat flux with mass velocity. Liquid hydrogen; test-section pressure, approximately 50 pounds per square inch absolute; average inlet sub-cooling, 20°R .



(c) Critical-boiling-length-to-diameter ratio, approximately 15.

Figure 6. - Continued. Variation of critical heat flux with mass velocity. Liquid hydrogen; test-section pressure, approximately 50 pounds per square inch absolute; average inlet sub-cooling, 2°R .



(d) Critical-boiling-length-to-diameter ratio, approximately 8.5.

Figure 6. - Concluded. Variation of critical heat flux with mass velocity. Liquid hydrogen; test-section pressure, approximately 50 pounds per square inch absolute; average inlet sub-cooling, 2° R.

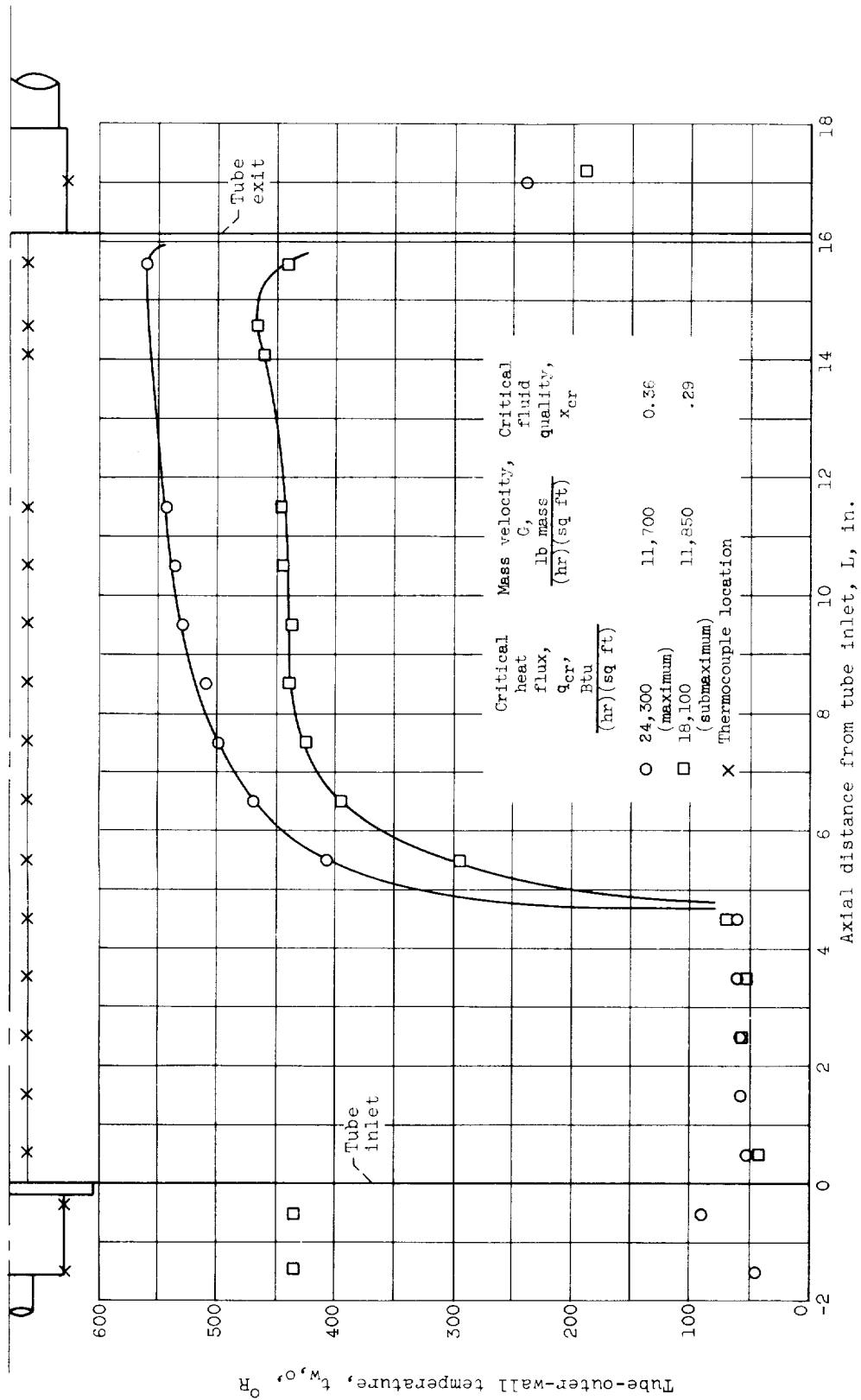


Figure 7. - Comparison of tube-outer-wall temperature profiles for maximum and submaximum critical heat-flux conditions. Liquid hydrogen; test-section pressure, approximately 50 pounds per square inch absolute; average inlet subcooling, 20 R.

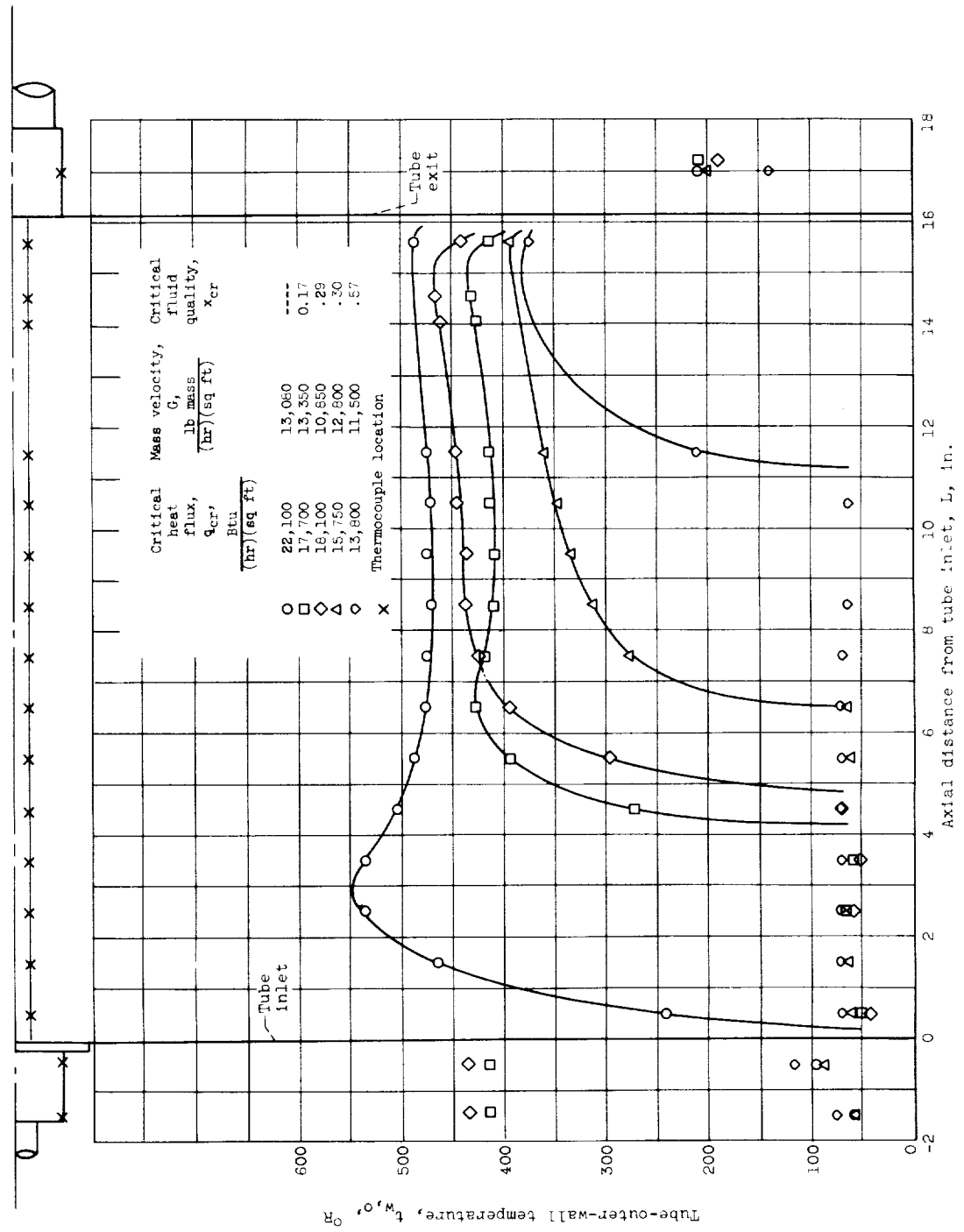
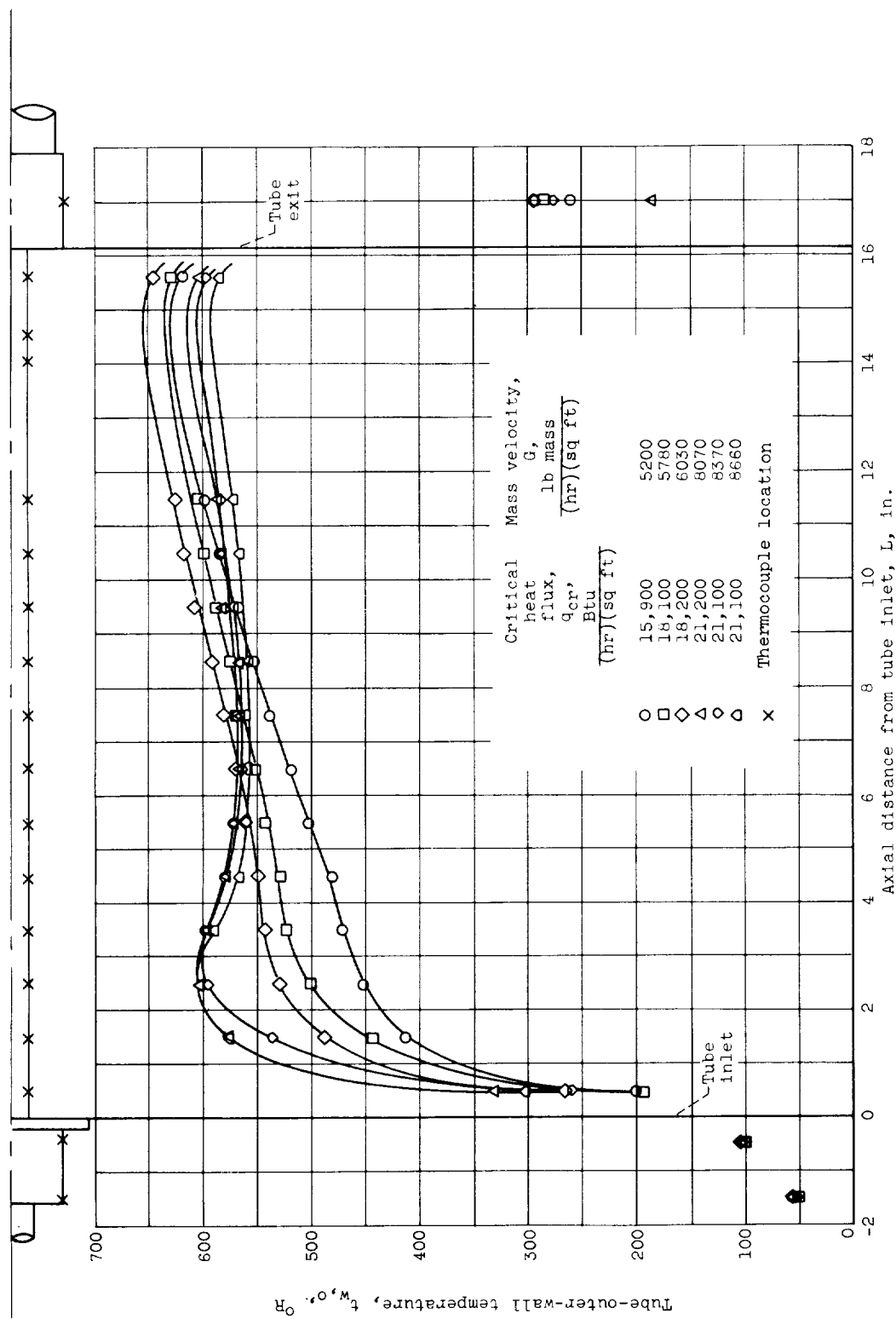
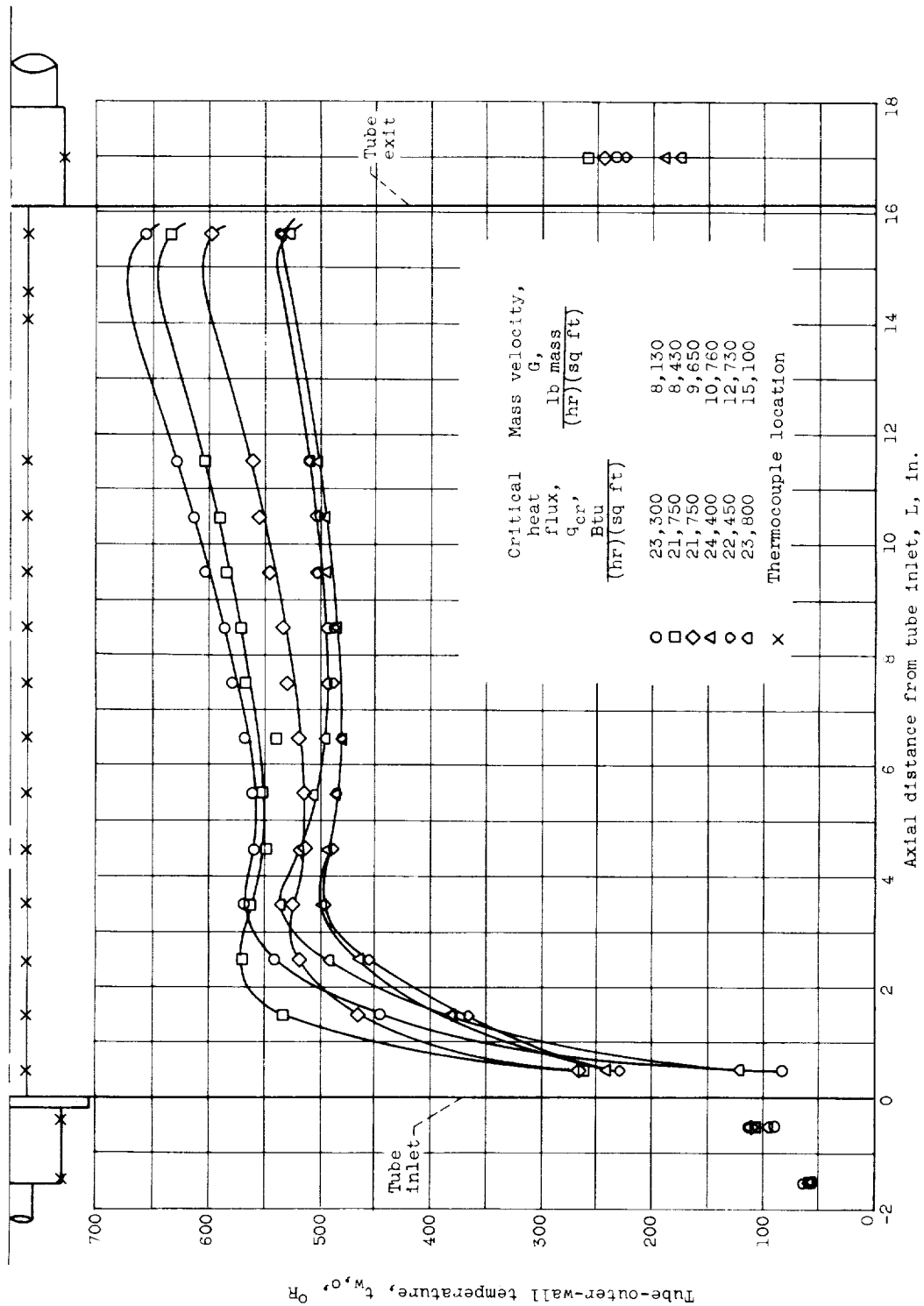


Figure 8. - Comparison of tube-outer-wall temperature profiles for submaximum critical-heat-flux conditions at various heat fluxes and constant mass velocity. Liquid hydrogen; test-section pressure, approximately 50 pounds per square inch absolute; average inlet subcooling, 2° R.



(a) Test-section pressure, approximately 50 pounds per square inch absolute.
Figure 9. - Tube-outer-wall temperature profiles for liquid hydrogen with wall temperature rise at tube inlet.



(b) Test-section pressure, approximately 70 pounds per square inch absolute.

Figure 9. - Concluded. Tube-outer-wall temperature profiles for liquid hydrogen with wall temperature rise at tube inlet.

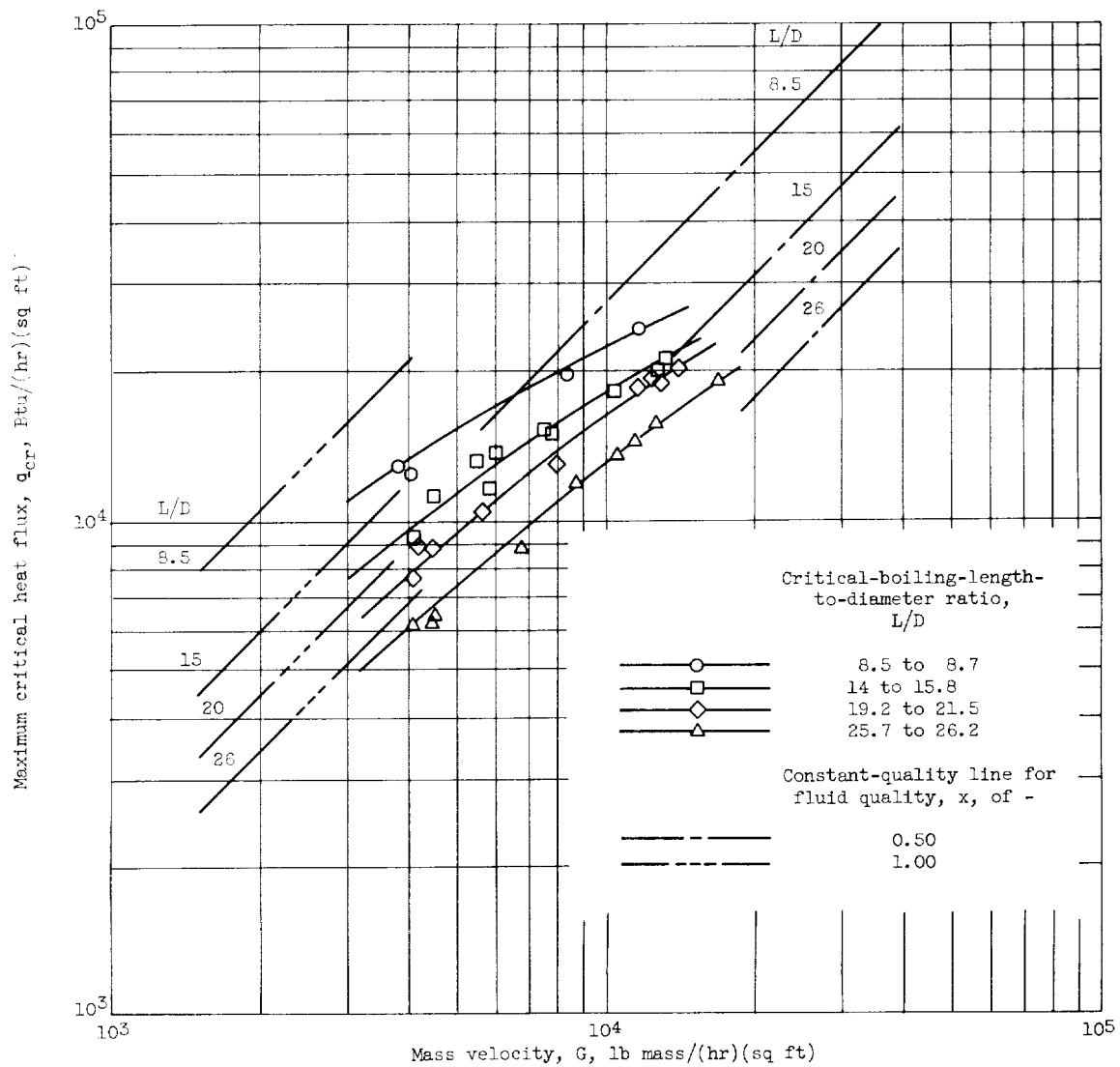


Figure 10. - Variation of maximum critical heat flux with mass velocity at various critical-boiling-length-to-diameter ratios. Liquid hydrogen; test-section pressure, approximately 50 pounds per square inch absolute; average inlet subcooling, 2° R.

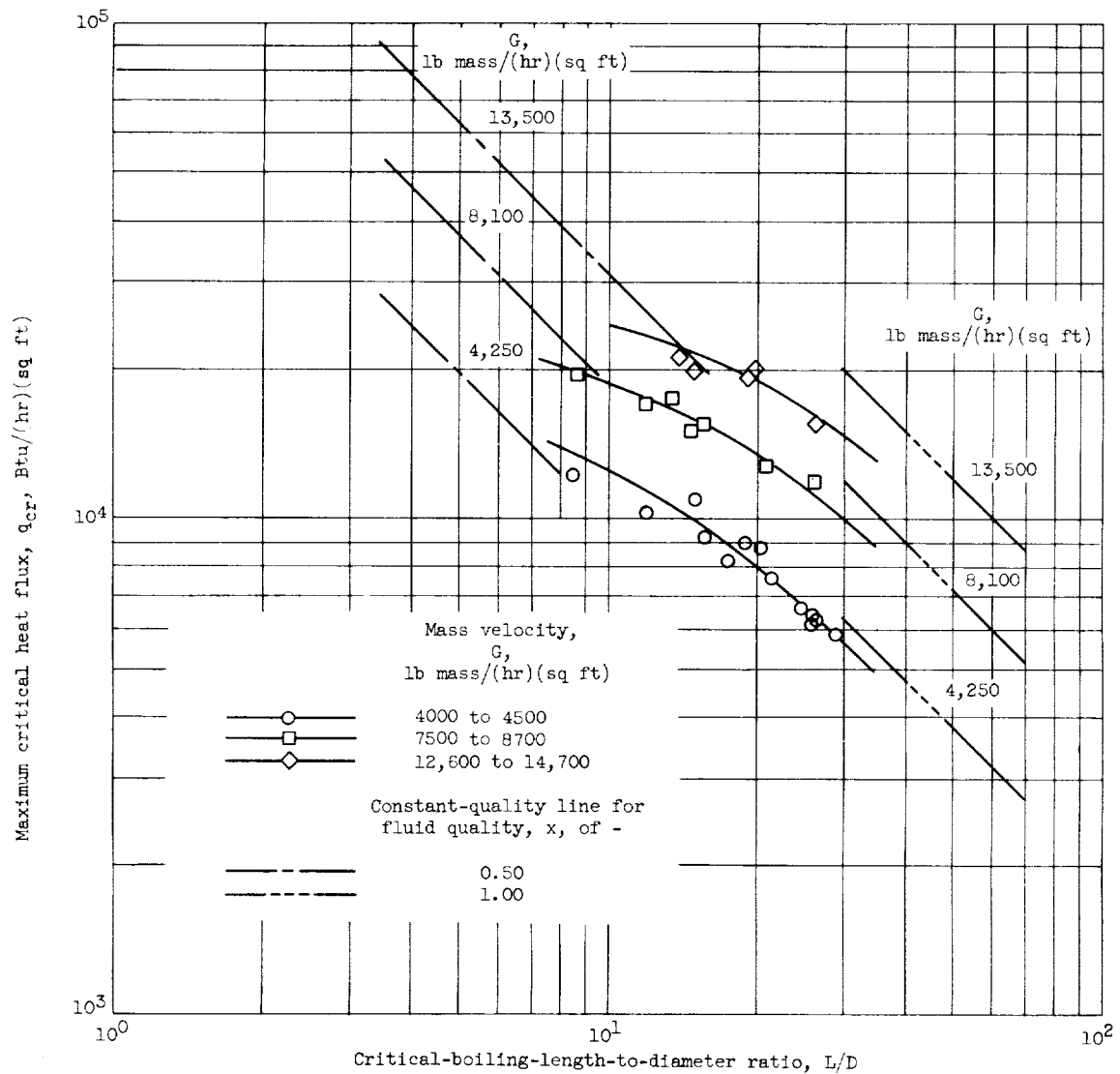


Figure 11. - Variation of maximum critical heat flux with critical-boiling-length-to-diameter ratio at various mass velocities. Liquid hydrogen; test-section pressure, approximately 50 pounds per square inch absolute; average inlet subcooling, 2° R.

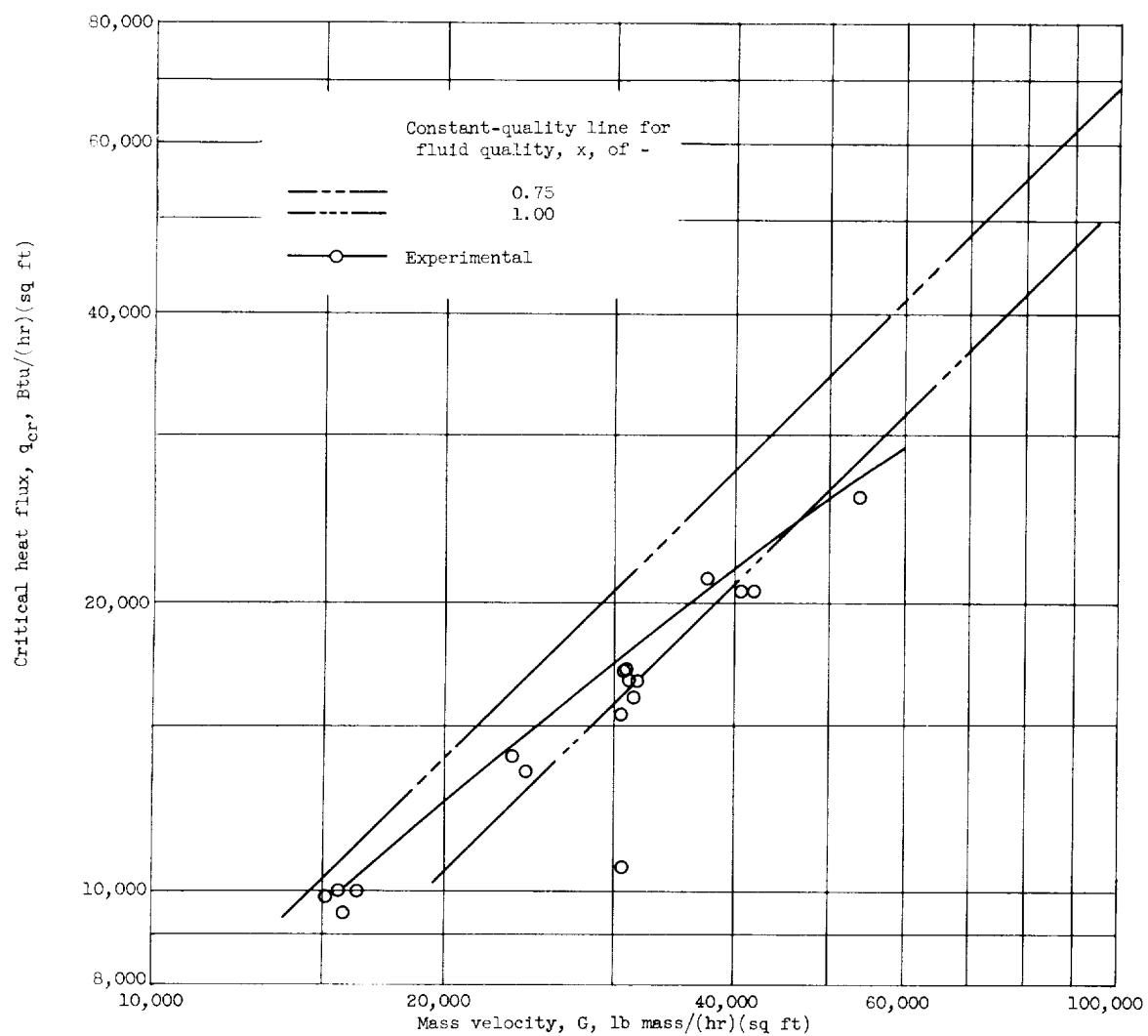


Figure 12. - Variation of critical heat flux with mass velocity at critical-boiling-length-to-diameter ratio of 29. Liquid nitrogen; test-section pressure, approximately 50 pounds per square inch absolute; average inlet subcooling, 4°R .

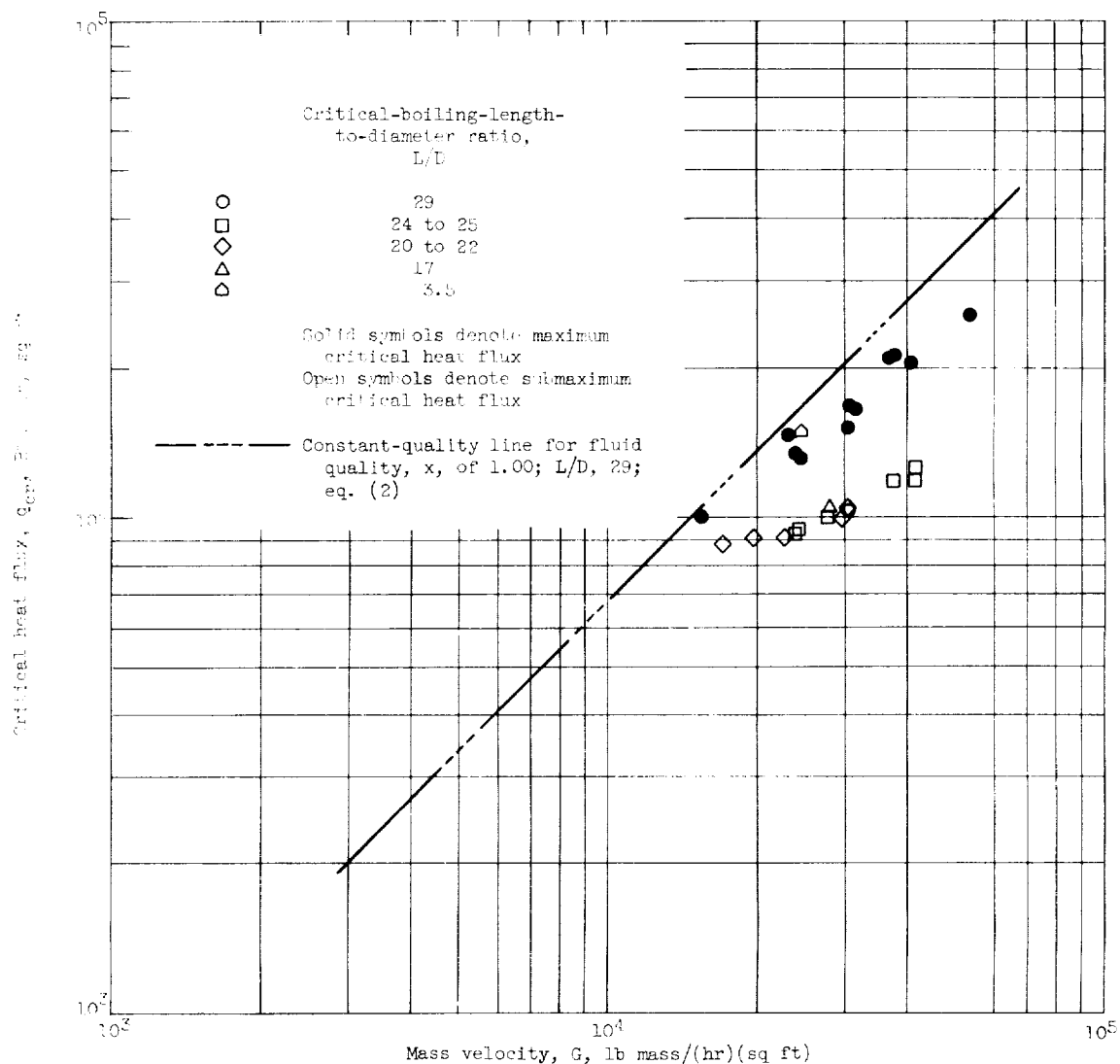


Figure 13. - Comparison of maximum critical boiling heat flux with submaximum critical boiling heat flux. Liquid nitrogen; test-section pressure, 48 to 53 pounds per square inch absolute; inlet subcooling, 10 to 60° R.

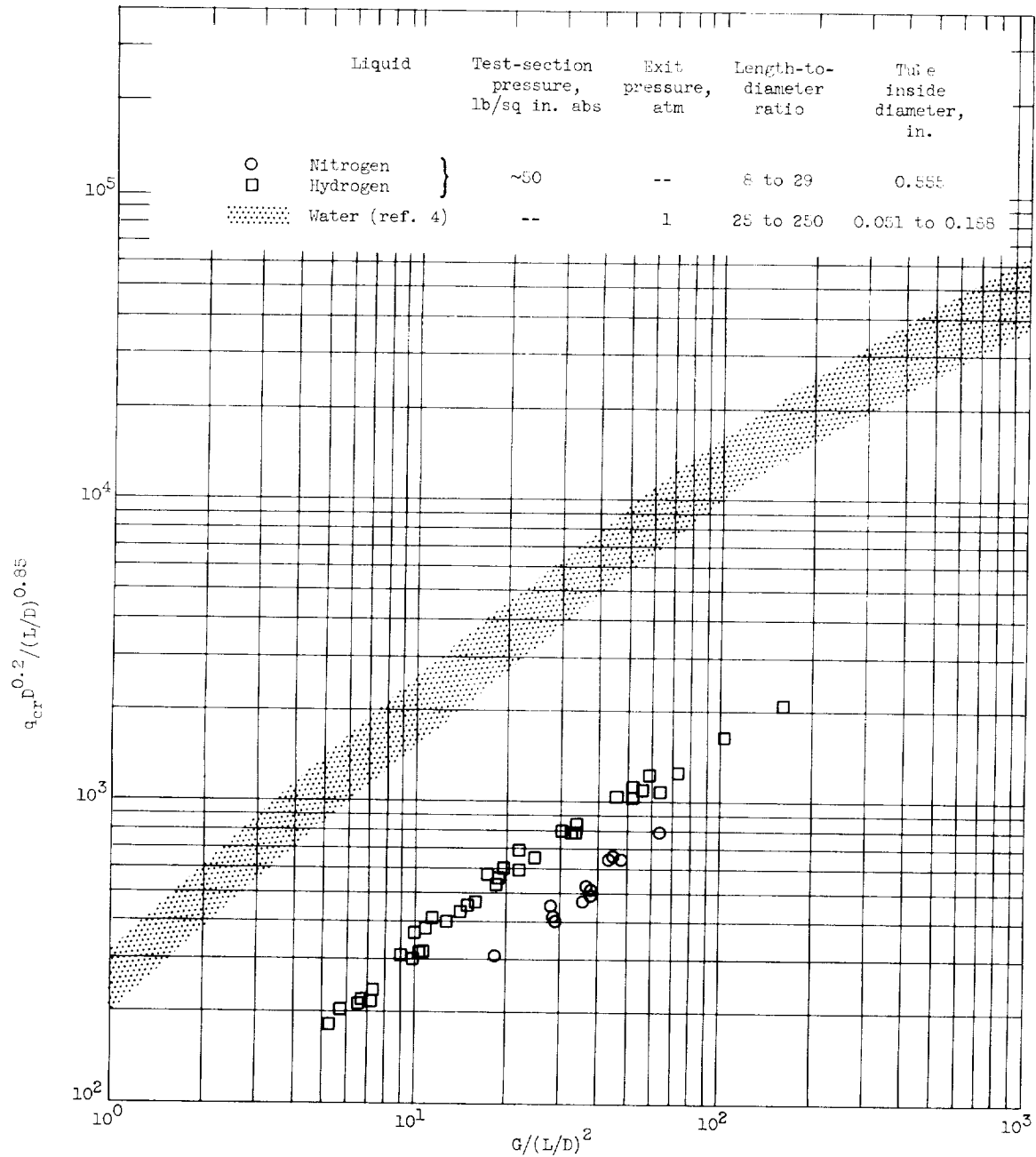


Figure 14. - Comparison of maximum critical heat flux for cryogenic liquids with water correlation of reference 4.

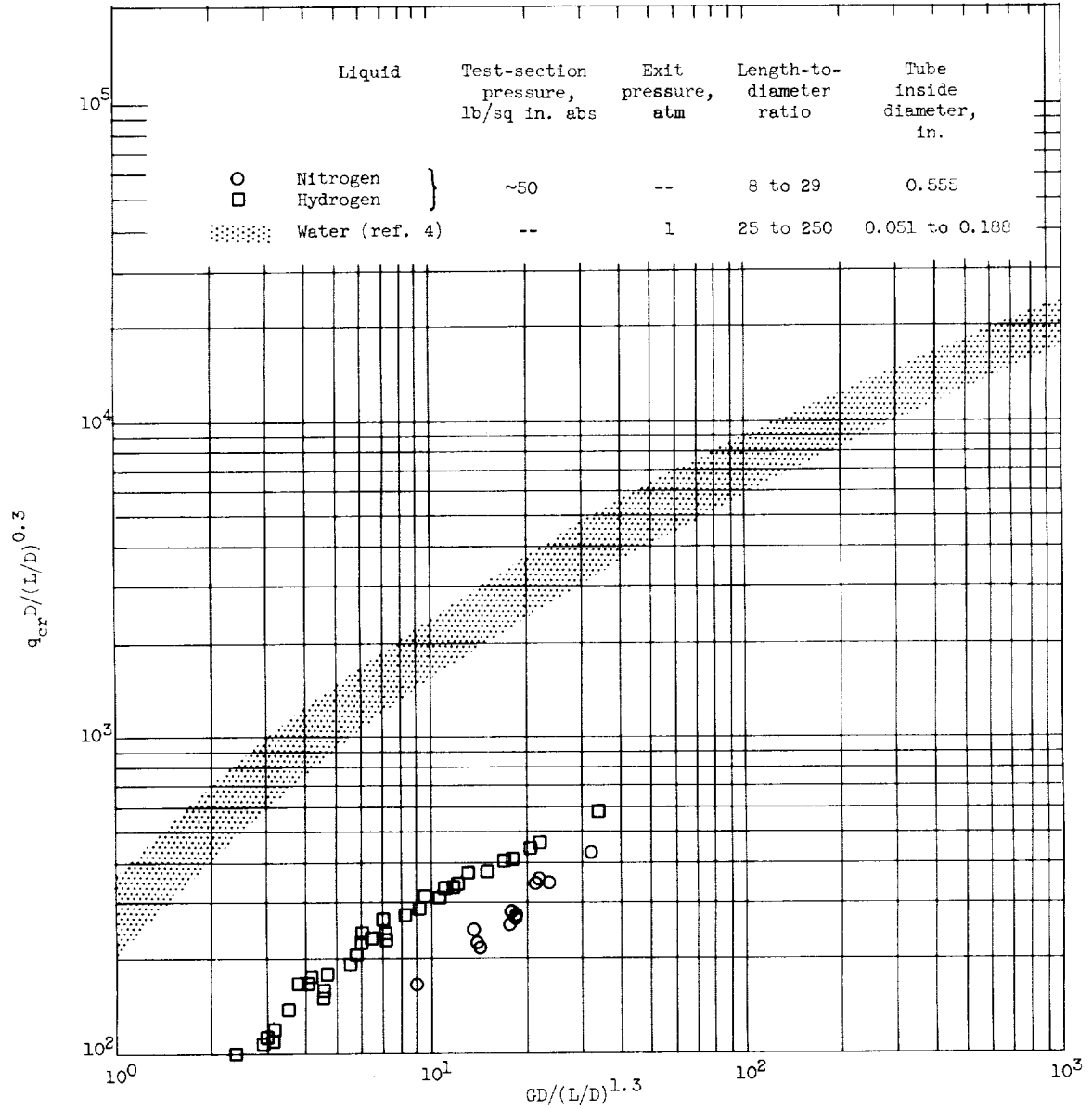


Figure 15. - Comparison of maximum critical heat flux for cryogenic liquids with water in terms of revised geometric parameters.

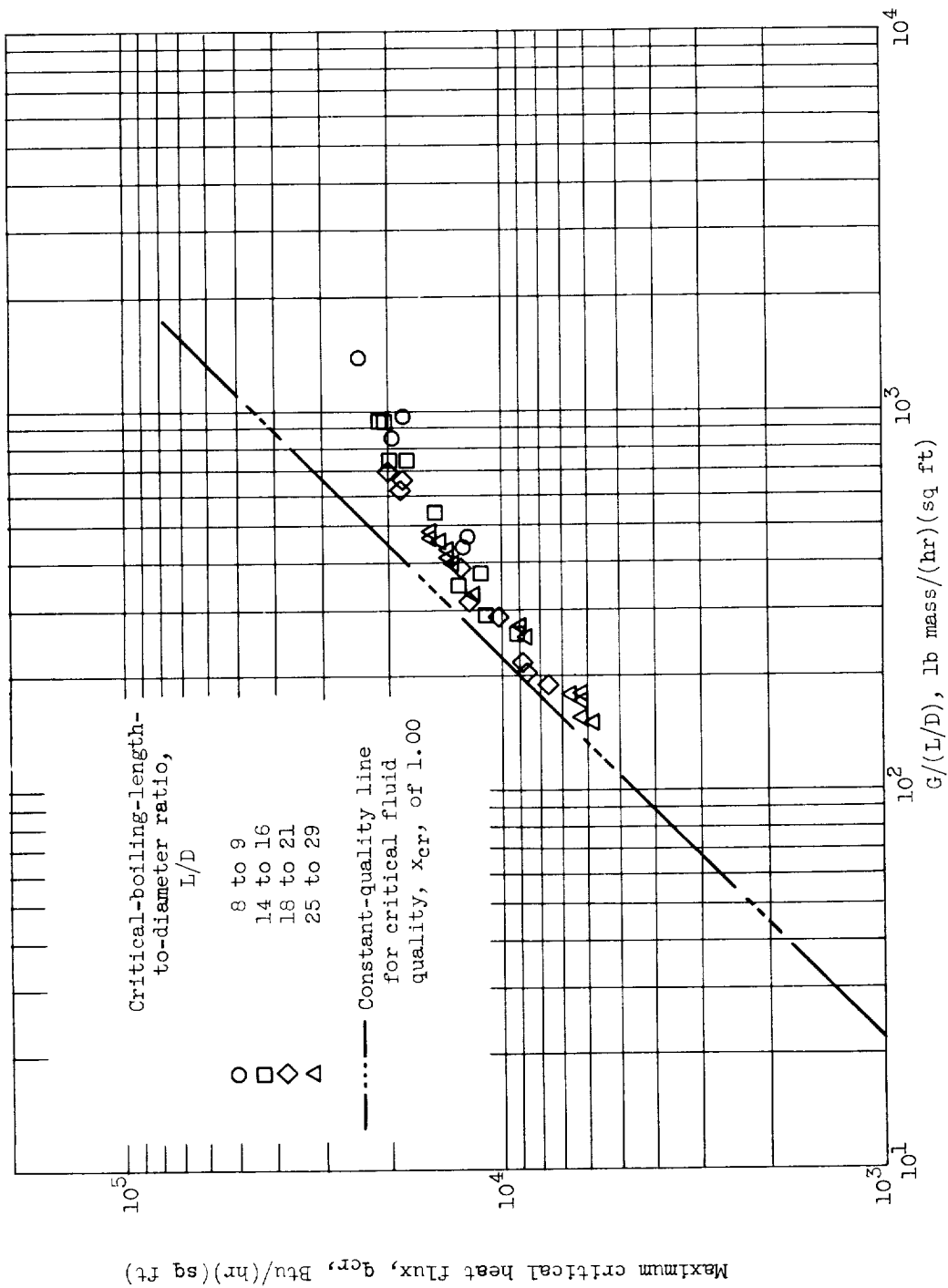


Figure 16. - Maximum critical heat flux as function of flow and length parameter. Boiling liquid hydrogen; tube inside diameter, 0.555 inch; test-section pressure, approximately 50 pounds per square inch absolute; average inlet subcooling, 20 R.

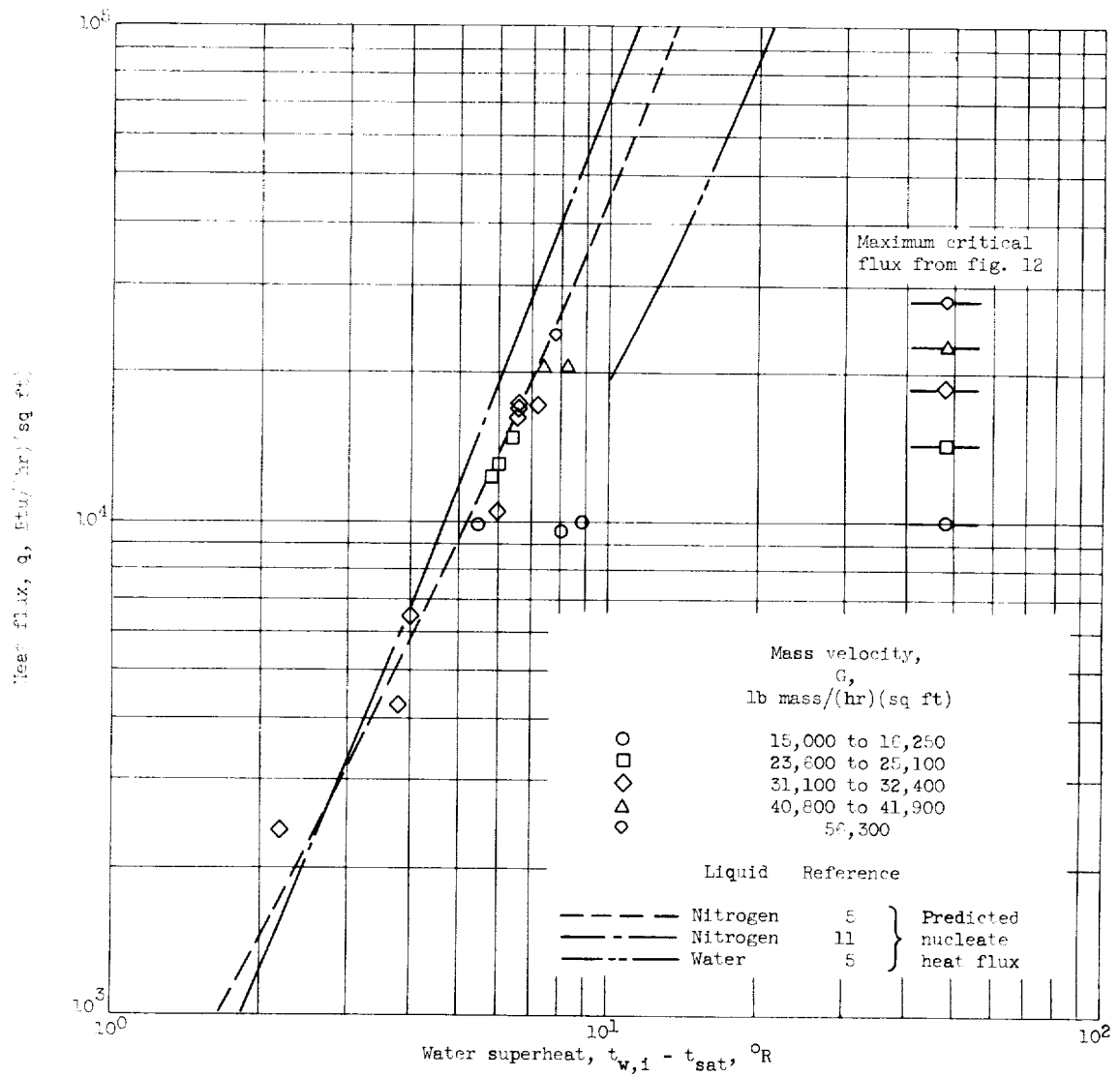


Figure 17. - Nucleate heat flux as function of wall superheat. Liquid nitrogen; test-section pressure, 48 to 56 pounds per square inch absolute; inlet subcooling, 3° to 5° R; length-to-diameter ratio, 29.

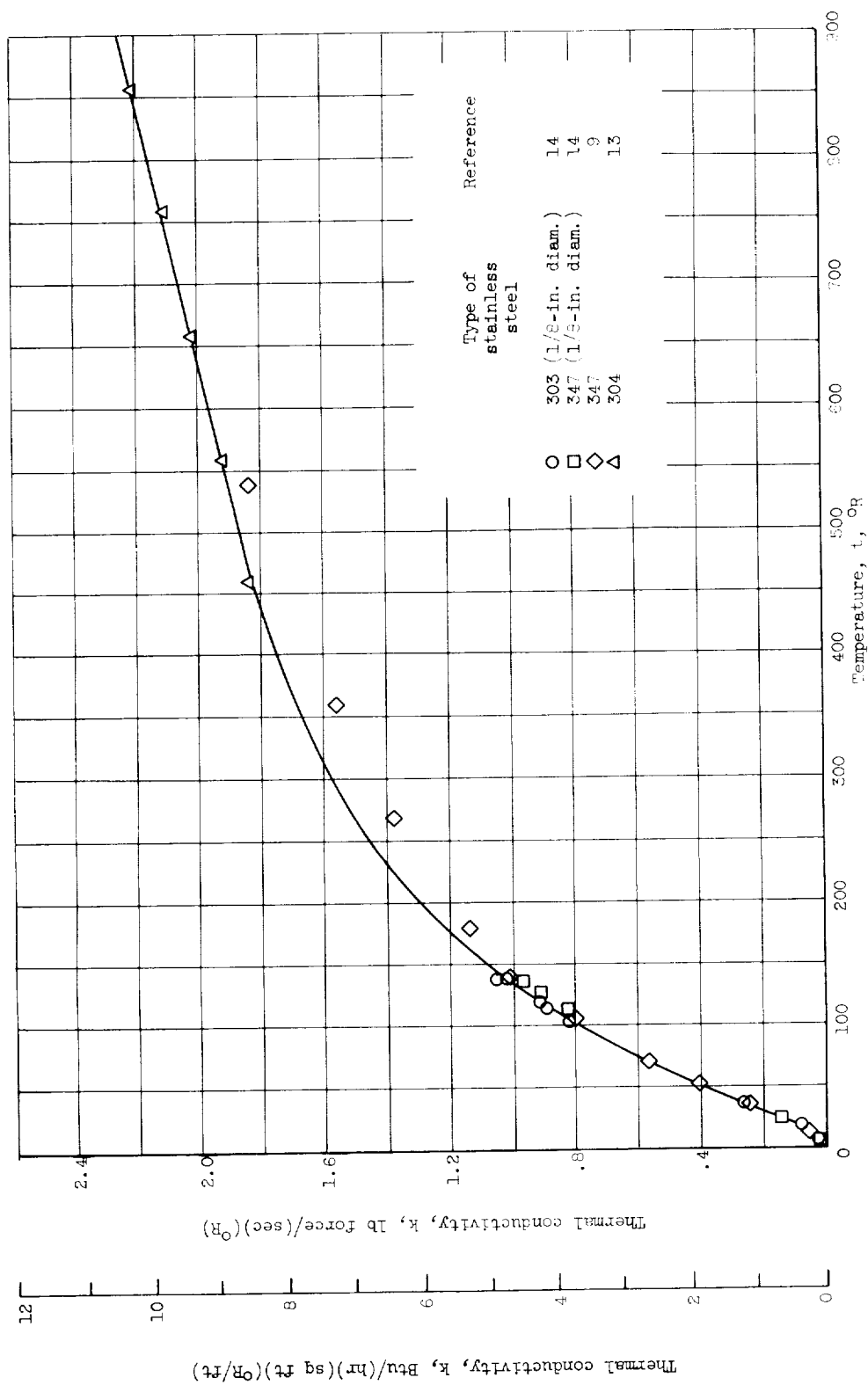


Figure 15. - Variation of thermal conductivity of 303, 304, and 347 stainless steel with temperature.

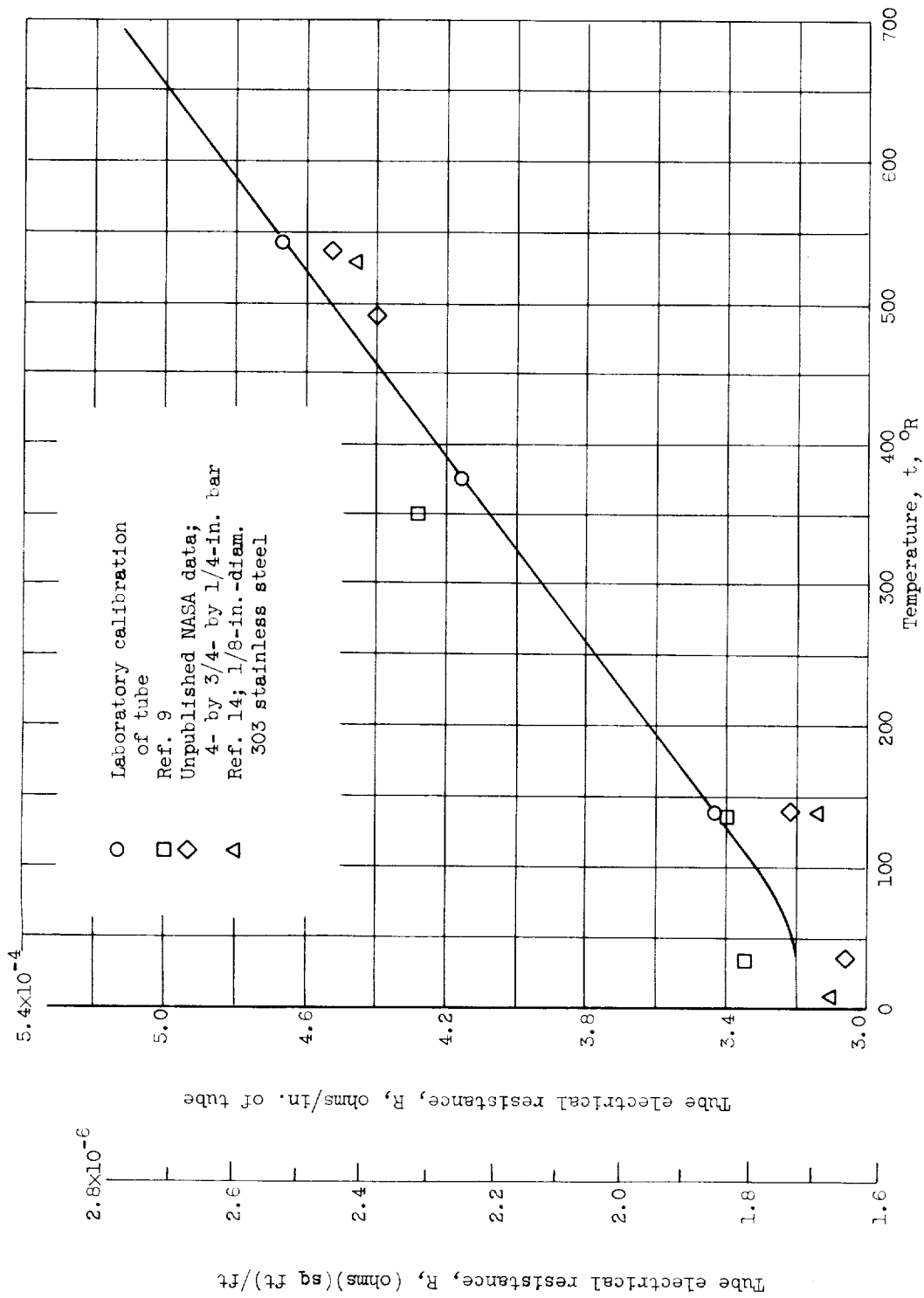
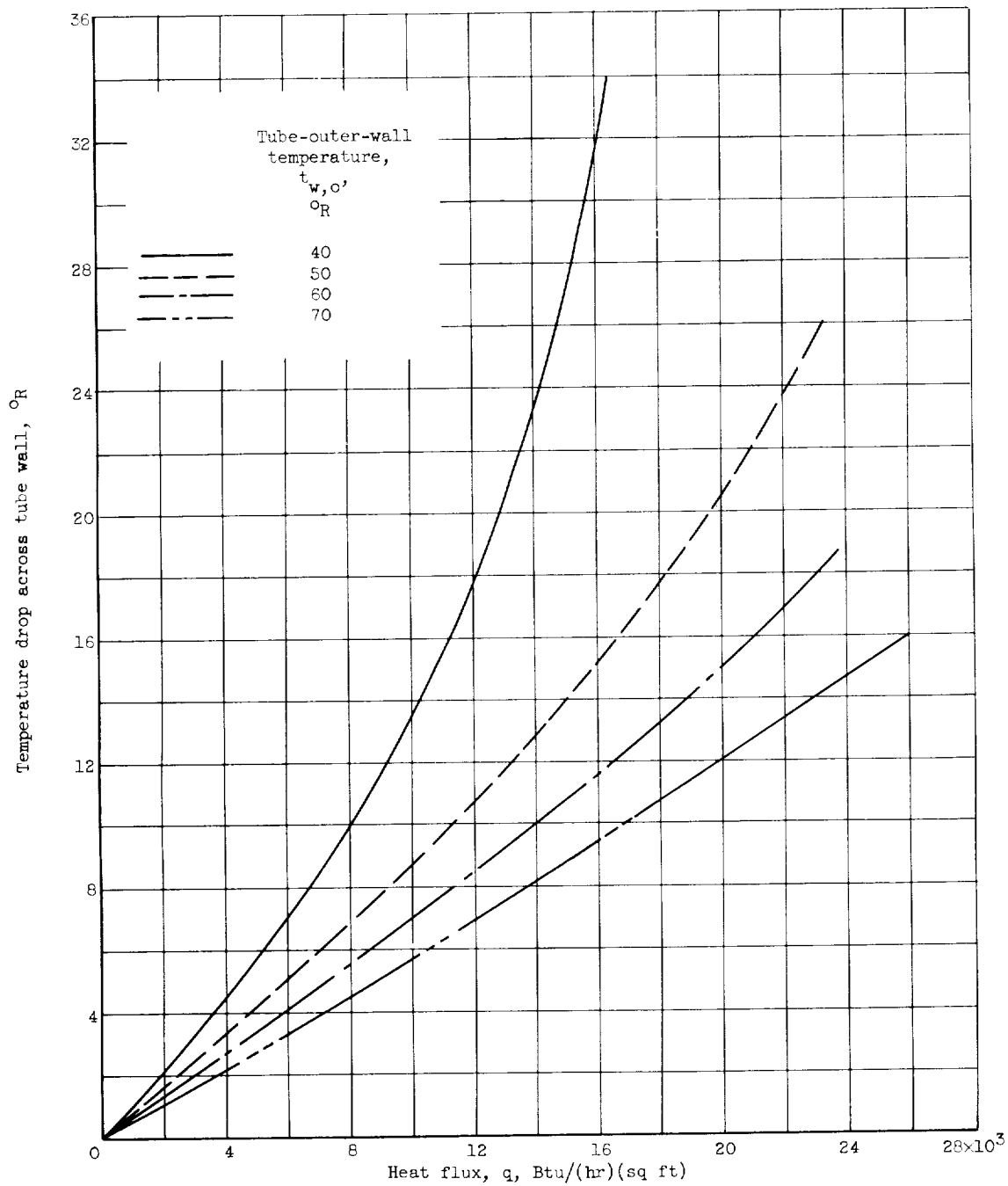


Figure 19. - Variation of tube electrical resistance with temperature. Tube of 304 stainless steel; outside diameter, 0.625 inch; inside diameter, 0.555 inch.



(a) Hydrogen test conditions.

Figure 20. - Temperature drop across tube wall as function of heat flux and tube-outer-wall temperature. Negligible axial temperature gradient; tube of 304 stainless steel; inside diameter, 0.555 inch; wall thickness, 0.035 inch.

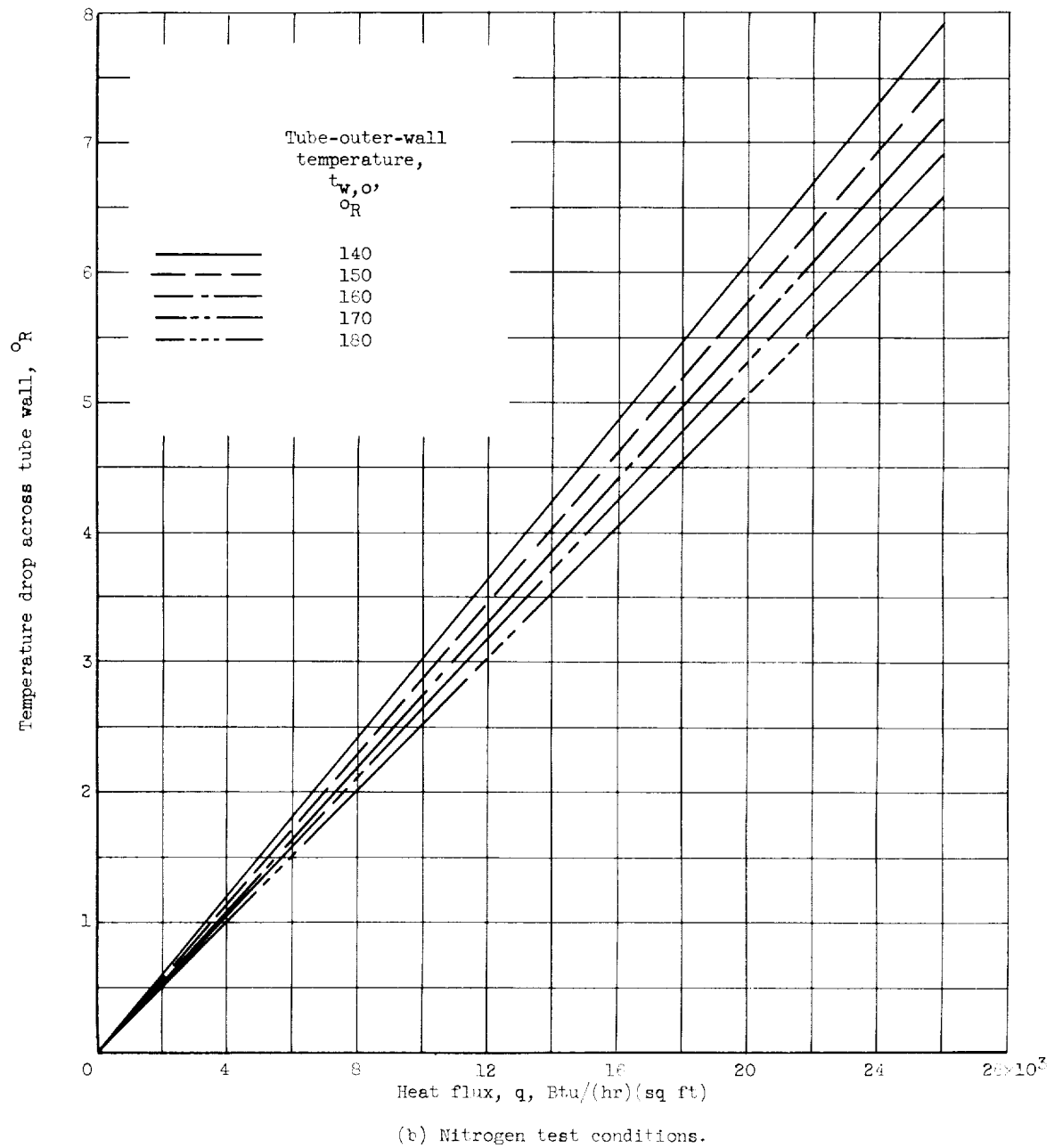


Figure 20. - Concluded. Temperature drop across tube wall as function of heat flux and tube-outer-wall temperature. Negligible axial temperature gradient; tube of 304 stainless steel; inside diameter, 0.555 inch; wall thickness, 0.035 inch.

